

高雄醫學大學暨中央研究院轉譯醫學博士學程
博士論文

**Ph.D. Program in Translational Medicine, Kaohsiung
Medical University and Academia Sinica
Doctoral Dissertation**

指導教授： 鐘育志 教授 Dr. Yuh-Jyh Jong
陳俊安 教授 Dr. Jun-An Chen

**MiR34 參與脊髓性肌肉萎縮症的致病機制，有
潛力成為第一型患者對Nusinersen療效的預測
性生物標誌**

**MiR34 Contributes to Spinal Muscular Atrophy
Pathogenesis and Potentially Serves as a
Predictive Biomarker for Nusinersen Response
in Type I Patients**

研究生：陳泰亨 Tai-Heng Chen

中華民國 112 年 5 月

Table of Contents

Chapter	Page
I、Content Index-----	1
II、摘要 Abstract	
II.1 中文摘要-----	4
II.2 Abstract-----	5
III、Acknowledgements(致謝辭) -----	7
IV、Background and Introduction-----	8
V、Materials and Methods	
Patients-----	16
Human Serum Collection for miRNA Profiling -----	18
Serum miRNA microarray profiling-----	18
pNfH measurement-----	20
Mouse breeding and maintenance-----	20
Study animal tissue collection-----	21
Mouse ESC culture and MN differentiation-----	22
Human ESC/iPSC culture and differentiation-----	23
microRNA <i>in situ</i> hybridization and miRNAscope assay-----	25

RNA isolation from CSF of SMA patients-----	27
RNA isolation and qRT-PCR-----	27
RNA-sequencing analysis-----	28
Immunostaining -----	30
Predicted MiR-34/449 target genes and gene ontology analysis---	32
scAAV9-MiR34a preparation and injection-----	32
Statistical analysis-----	33
Data Availability Statement-----	34

VI • Results

Serum MiRNA profiling to identify candidate biomarkers-----	35
Identification of MiRNAs as candidate biomarkers through spinal MNs-----	36
Early dysregulation of MiR34 among SMA patient iPSC-differentiated MNs-----	39
Validation of spinal miRNA dysregulation in SMN Δ 7 mice during the critical window for intervention-----	41
The MiR34 family regulates motor-end plate function of neuromuscular junction-----	43

MiR34 family regulates synaptic formation pathways-----	46
Introduction of MiR34a in the neonatal period partially alleviates the severity of SMN Δ 7 mice-----	47
MiR34 in the cerebrospinal fluid predicts the treatment response of nusinersen in type I SMA patients-----	49
VII 、 Discussion-----	53
VIII 、 Conclusions-----	75
IX 、 Figures and Tables -----	76
X 、 References -----	96
XI 、 Appendix-----	110

共（123）頁

II. 摘要 ABSTRACT

II.1 中文摘要

脊髓性肌肉萎縮症 (SMA) 起因於脊髓運動神經元凋亡造成肌肉萎縮。SMA 致病機轉是由 *SMN1* 基因的缺損造成其產物運動神經元存活蛋白 (SMN) 的缺乏。微小核糖核酸 (miRNAs) 是一種調節轉錄後基因表達的非編碼 RNA，近來研究顯示 miRNAs 有潛力作為運動神經元疾病的生物標誌物。此研究旨在探尋參與 SMA 致病機轉的 miRNAs，且有潛力作為生物標誌用來預測病患對 nusinersen 治療反應。實驗結果發現 MiR34 在 SMA 人類細胞和老鼠模式顯著下降，並且在 *Mir34* 家族剔除的基因小鼠的神經肌肉鍵結 (NMJ) 中，也出現類似 SMA 老鼠 (SMN $\Delta 7$) 的病理變化。利用病毒載體注射 MiR34a 至 SMN $\Delta 7$ 小鼠，可以改善 NMJ 的病理缺損與其運動功能。在 nusinersen 治療的初始導入劑量階段，第一型 SMA 患者腦脊髓液 (CSF) 中 MiR34 出現下降趨勢，並且在給藥前的 MiR34 定量或可預測一年後患者的運動改善程度。此研究顯示 MiR34 可能作為 SMA 的潛在生物標誌，因其參與 SMA 的病理機轉，而病患 CSF 中 MiR34 表現量有潛力作為 nusinersen 療效的指標，往後或許可提供臨床端對 SMA 治療決策的參考。

中文關鍵詞：脊髓性肌肉萎縮症；微小核糖核酸；腦脊髓液；療效指標

II.2 英文摘要 Abstract

Spinal muscular atrophy (SMA) is caused by the progressive death of spinal motor neurons, leading to muscle wasting. It is primarily due to a deficiency of the survival motor neuron (SMN) protein, which results from defects in the *SMN1* gene. MicroRNAs (miRNAs) are non-coding RNAs that regulate gene expression post-transcriptionally and have recently shown promise as biomarkers for motor neuron diseases. This study investigated the involvement of miRNAs in SMA pathogenesis and their potential as biomarkers for predicting patient responses to nusinersen treatment. The results showed a significant decrease in miR34 levels in SMA human cells and mouse models. Similar pathological changes to those found in SMA mice (SMN Δ 7) were also observed in the neuromuscular junction (NMJ) of *Mir34* family-knockout mice.

Introducing MiR34a to SMN Δ 7 mice via viral vectors improved NMJ pathology and motor function. In type I SMA patients, MiR34 levels in the cerebrospinal fluid (CSF) declined during the loading phase of nusinersen treatment. The baseline level of MiR34 before treatment may predict motor improvement one year later. This study suggests that

MiR34 could serve as a potential biomarker for SMA, as it is involved in the disease's pathological mechanism. Furthermore, MiR34 expression in patients' CSF could be used to predict nusinersen treatment efficacy, providing valuable information for future SMA treatment decisions.

Keywords: spinal muscular atrophy, nusinersen, microRNA, biomarker,

MiR34



Acknowledgements

約莫二十年前的夏夜，凌晨兩點到巴士站坐夜車前往台北，為的是隔天早上可以趕赴中研院，解剖分析全世界第一隻 SMA 老鼠的脊髓神經構造，那是醫學生時期的我，這一切也彷彿歷歷在目。而這論文讓我有機會再次親自參與 SMA 研究並將結果整理出付梓，能一窺這難得的整合型實驗的奧妙，真是我莫大的福氣！

參與這試驗的 SMA 病友與家屬們，需向您們致上最高敬意，您們個個都是我所見過最偉大的生命勇士，您們的奉獻成就出此次試驗的結果，對於全世界的 SMA 患者提供極佳的數據，尤其在鐘育志教授領導的高醫大 SMA 照護團隊，提供給病友們最完善的照護，讓病患的檢體得到嚴密的保護與精確分析，相信您們的付出必將在 SMA 治療藥物研究發展史上留下重大貢獻的軌跡！

當然，如此需龐大人力物力且設計縝密的試驗，絕不是我一人可以完成，背後有賴於優異的研究團隊成員執行高效率與完美的配合，與兩位指導教授悉心的指導，在此容我一一感謝的是：陽明交通大學醫學院藥理所邱士華教授、資訊學院資工系洪瑞鴻教授、陳俊安老師實驗室的世欣、聿富、雅萍、彥中、揚明、賀強、怡靜。您們是我所見過最優秀的老師，長輩與同仁，自己感到非常榮幸可以身處在這團隊中，要沒有您們，這篇論文與我們所投稿到期刊的文章不會有如此好的進展。

最後，也將此論文獻給我的親愛的家人，您們的體諒與支持是不停促使著我在這漫漫的醫學研究的路上，可以充滿感恩地一直前行。

本研究榮獲財團法人罕見疾病基金會
「第十九屆罕見疾病博碩士論文獎助學金」獎助

謹於此特別致謝

IV. Background and Introduction

Spinal muscular atrophy (SMA), a leading genetic cause of worldwide infant death, is an autosomal recessive neurodegenerative disease characterized by relentless muscle wasting resulting from progressive spinal motor neuron (MNs) death. The genetic pathogenesis of SMA was first identified in 1995, reporting involvement in the defect of a functional survival motor neuron 1 (*SMN1*) gene. Deletion or mutation of the *SMN1* gene leads to decreased production of full-length (FL) survival motor neuron (SMN), a vital protein contributing to the function and survival of MNs. However, *SMN2*, a unique hypomorphic paralogue that shares 99% sequence identity with *SMN1*, possesses a C-to-T nucleotide variant in exon 7, leading to the exclusion of this exon during SMN transcript production [1]. Only ~ 10% of *SMN2* transcripts are complete (FL-*SMN2*) and translated into functional SMN protein [2]. While these FL-*SMN2* transcripts can partially compensate for the loss of *SMN1*, it is reasoned that retained *SMN2* copy numbers of patients determine the phenotypic severity [2-4]. However, such phenotype-genotype correlation based on various *SMN2* copy number is not absolute and is usually affected by

other disease-modifying factors. Multifaceted roles of SMN protein are still under investigation, and it is unclear how a deficiency in ubiquitously expressed SMN can selectively cause dramatic MN degeneration [5]. Cell-autonomous effects related to SMN deficiency are responsible for the degeneration of MNs; however, these effects alone do not account for the entire SMA phenotype. This suggests that dysfunction in neural networks and the involvement of other cell types also play a role in the disease process of SMA [6,7]. Indeed, increasing evidence extend the SMA pathological change may beyond MNs to include additional cells both within and outside the central nervous system (CNS), whereby numerous peripheral organs and non-neuronal tissues, such as neuromuscular junction (NMJ) and muscles [8].

Since identifying the causal relationship between SMN loss and SMA phenotypes, many treatment strategies have focused on restoring SMN levels. SMA phenotypes are partially mitigated by the low levels of SMN protein produced by varying numbers of SMN2 copies. This limited expression of SMN protein offers an ideal therapeutic target for SMA

treatment [9]. Following this proof of concept, all currently available FDA-approved treatment for SMA are based on enhancing the SMN-dependent pathway, including intrathecal delivery of splicing-corrective antisense oligonucleotide (ASO) Nusinersen/Spinraza® [10-13], onasemnogene abeparvovec representing *SMN* gene therapy delivered by self-complementary adeno-associated virus (scAAV) [14,15], and oral Evrysdi® (risdiplam) acting as a splicing modifier to promote *SMN2* exon 7 inclusion [16,17]. These therapies have exhibited promising outcomes in most treated SMA patients, especially those with severe type I who have undergone a newborn screening program. This emerging array of therapeutic options with distinct modes of action enables personalized treatment protocols for optimal prognoses. However, emerging clinical data indicate that not all treated SMA patients responded equally well to these novel therapies. There are several factors proposed to influence these variable responses. One of the most important factors is the time between the first symptoms presentation and the therapy initiation, known as the therapeutic window [18]. Two other response-confounding factors recently proposed on

patient evolution: the disease duration [19] and the baseline status [20]. In addition, several genetic modifiers are known to regulate *SMN* transcription, splicing, and mRNA stability [21-24], which might explain why *SMN2* copy number does not always precisely predict disease severity, despite being the sole source of SMN protein in SMA patients [25]. These genetic modifiers could interact with currently available medications, resulting in distinct patient responses [26,27]. Considering the broad heterogeneity of clinical phenotypes of SMA, a uniform dose and equal dosing intervals across all patients seem impractical for the therapeutic strategy. Especially in the SMA condition, the main affected cell type and the primary target of SMN-restoring therapies are spinal MNs, which are rarely accessible for patient quantity measurement [28]. Therefore, potential biomarkers that can reliably predict and monitor treatment responses are sorely needed to facilitate the choice of therapeutic plans and enable timely adjustment during the treatment course [29,30].

MicroRNAs (miRNAs) are a class of short, non-coding RNA molecules

that play a pivotal role in regulating gene expression. They typically bind to messenger RNA (mRNA) to fine-tune gene expression by controlling the translational efficacy in response to changing conditions. What makes miRNAs particularly intriguing is their tissue-specific expression patterns. Unlike protein-coding genes, miRNAs are typically expressed in specific tissues. This character allows them to modulate gene expression in a tissue-specific manner, contributing to the overall robustness of the regulatory networks that control cellular function [31,32]. As a result, such tissue-specific expression is that disease-linked miRNAs are often dysregulated in a tissue or cell-type-specific fashion. For example, many miRNAs have been dysregulated in MN diseases such as amyotrophic lateral sclerosis (ALS) [33-35] and SMA [36-38]. In motor neuron diseases, miRNAs play a significant role at the molecular pathology level, actively regulating crucial aspects of the disease, including cell death, neurite outgrowth, and excitotoxicity [34,35,39,40]. Despite being expressed primarily in specific cell types, miRNAs are not limited to their host cells, as they can participate in intercellular communication. Some miRNAs are actively sorted and packaged for exocytosis in various cell

types [41-43], and miRNA-containing extracellular vesicles can be taken up by other cells, where they regulate target genes in the recipient cell [44]. Because miRNAs are tissue-specific, directly involved in the disease process, and extracellular presence, they are critical to understanding the molecular basis of diseases and represent promising biomarkers to reflect disease progression and predict prognosis [36,45]. Recent transcriptome studies have also identified several specific miRNAs involved in survival, synaptic plasticity/formation, endoplasmic reticulum stress, and ribosomal RNA binding in different SMA animal and cell models [46]. It is known that miRNAs can be actively secreted from a cell or leaked through the membrane, resulting in detectable level changes in various biofluids with relative stability - such as cerebrospinal fluid (CSF), serum/plasma, saliva, and urine [47]. Besides, due to the nature of multifaceted functions in regulating both MN and non-MN tissues, miRNAs have the advantage of being able to detect changes in levels across multiple tissues, making them valuable tools for monitoring therapeutic response. As a result, miRNAs can be applied as potential biomarkers non-invasive to monitor disease progress and treatment

response. This characteristic is a significant advantage because it allows real-time therapeutic response monitoring and can help guide treatment decisions. As such, miRNAs are promising candidates for personalized medicine approaches in the therapeutic era of SMA [37,48-50].

Although rigorous studies have been conducted to identify biomarkers of SMA in patients and/or animal models that reflect disease severity and treatment responses [28-30], they have only had limited success, and their reliability remains controversial. This could be attributed to the nature that miRNAs in biofluids might fluctuate associated with gender, age, and metabolism; thereby, the expression change of the expression of miRNA in biofluids might not faithfully reflect SMA pathology. Thus in the present study, we aimed to systematically investigate potential miRNAs that reflect both the physiology and pathology of MNs to identify candidate biomarkers that could be applied to predict the efficacy of SMA treatment. We tried to expand our search beyond the canonical biomarker candidates, such as circulating proteins, and explore other promising biomarkers that could provide more specific and accurate information. By

investigating the role of miRNAs in MNs, we sought to identify bona fide biomarkers that could predict therapeutic responses and improve clinical decisions on a treatment course for SMA patients [38,51]. Furthermore, despite the invasive nature of obtaining such tissue, we focused on spinal cord tissue in our biomarker search. This approach is because MN of the spinal cord is a primary site of pathology in SMA and may contain unique miRNA signatures that reflect disease progression and therapeutic response.



V. Materials and Methods

Patients

We conducted a study involving a consecutive cohort of seven type I SMA patients (four females and three males, respectively), all clinically diagnosed and genetically confirmed to have *SMN1* deletion/mutation. These SMA patients were treated with nusinersen at Kaohsiung Medical University Hospital, following the standard protocol issued by the manufacturer. We collected the patients' baseline demographics and clinical motor function data during each hospital visit using the Hammersmith Infant Neurological Examination (HINE-2) scores. HINE-2 is a quantifiable scale that measures motor function development by assessing the achievement of motor milestones such as voluntary grasp, kicking, head control, rolling, sitting, crawling, standing, and walking. HINE-2 scores range from 0 to 26, with higher scores representing better motor function [52]. This study defined a positive treatment response as patients demonstrating improvement in at least one motor milestone or having more milestones with improvements than declining performance. We compared targeted

molecular biomarkers, such as pNfH and MiR34, with HINE-2 motor performance measurements taken at day 0 (before initiating nusinersen treatment) and on days 64, 183, and 482 after nusinersen administration. CSF samples were collected from the patients, frozen at -80 °C, and diluted to the minimum required concentration using an assay dilution buffer prior to use. The Institutional Review Board of Kaohsiung Medical University Hospital (KMUHIRB-SV(I)-20170041) and Academia Sinica (AS-IRB01-12174, AS-IRB01-15046, AS-IRB01-17021, and AS-IRB01-18015) approved the study, and informed consent had been obtained from the guardians of all participating type I SMA patients. By examining the correlation between treatment response and biomarker levels, this study explored the potential of targeted biomarkers like pNfH and MiR34 as potentially reliable motor function indicators in type I SMA patients receiving nusinersen treatment. For the miRNA profiling in serum samples, we collected serum from five healthy individuals and SMA patients (2 type III, 2 type II, and 1 type I), respectively. Among the five SMA patients, their genotypes all showed 3 *SMN2* copies (*SMN1*: *SMN2*: 0:3).

Human Serum Collection for miRNA Profiling

After obtaining proper consent, 10-15 ml of blood (6-10 ml if the patient is younger than two years old) was collected from each patient in a spray-dried EDTA tube. The blood sample was then incubated at room temperature for 30 minutes for coagulation. The clot and cellular component were separated by centrifuging the sample at 400x g. The supernatant was transferred to a new vial and stored at -80°C before RNA extraction. RNA extraction was performed for serum samples using the miRCURY RNA Isolation Kit – Biofluid (Exiqon) following the manufacturer's instructions. Custom miRCURY microRNA panels were designed to validate candidate miRNAs identified in previous microarray profiling.

Serum miRNA microarray profiling

For miRNA analysis, a suitable assay, such as the TaqMan Array Human MicroRNA A+B Cards Set v3.0 (4444913, Thermo Fisher Scientific), would be employed to evaluate the miRNA profile. Total RNA isolated

from control and patients' serum samples would be extracted following the provided protocol. Log2-transformed data would then be normalized across samples by applying a scaling factor and adding a constant to median-filtered data to eliminate outliers. Passenger strands of miRNA and miRNAs with expression levels below five would be filtered out from the probe list, after which a differential expression analysis would be conducted. The quantity and quality of isolated RNA would be assessed using a spectrophotometer. Several unique probes for mature miRNAs would be assayed based on the miRNA database. Background subtraction would be applied to the raw data. A probe signal value would be considered detectable if it met three conditions: (1) signal intensity more than three times the background standard deviation, (2) spot coefficient of variation (CV) less than 0.5, with CV equal to the standard deviation divided by signal intensity, and (3) miRNAs classified as detectable if at least 50% of their repeating probes exceeded the detection level. Detectable signals would be normalized to eliminate system-related variations using a cyclic loess approach. Statistical comparisons between various groups would be conducted

using Student's t-test for independent samples, as appropriate. Differences would be deemed significant when p-values were less than 0.05.

pNfH measurement

To accurately measure the levels of phosphorylated neurofilament heavy chain (pNfH) of CSF, we utilized a high-quality, commercially available enzyme-linked immunosorbent assay (ELISA) kit from a reputable source (Euroimmun, Lubeck, Germany). By adhering to the manufacturer's detailed instructions and guidelines, we ensured the reliability and validity of the results obtained.

Mouse breeding and maintenance

In this study, we utilized heterozygous breeder pairs of a spinal muscular atrophy-like model, SMN Δ 7 mice (*Smn*^{+/-}; *SMN2*^{+/+}; *Smn* Δ 7^{+/+}) (VB.Cg-*Grm7*^{Tg(SMN2)89Ahmb} *Smn1*^{tm1Ms} Tg(*SMN2**delta7) 4299Ahmb/J, Stock #005025) imported from Jackson Laboratory. We also employed Mir34/449 triple knockout (TKO) mice, which were generated in the

C57BL/6J background, as reported previously [53]. To maintain and breed the mutant mouse lines, we conducted intercross mating between *Smn*^{+/-}; *SMN2*^{+/+}; *Smn*Δ7^{+/+} and *Mir34a*^{-/-}; *Mir34bc*^{+/-}; *Mir 449*^{-/-} mice. Unless otherwise stated, the control (Ctrl) group for all experiments consisted of age-matched littermates from these matings. Genotyping was carried out using the primers detailed in Table 1. In accordance with the 3Rs principles (Replacement, Reduction, and Refinement), we utilized the smallest possible sample size that would still yield statistically significant differences in the outcomes. The animals in this study had not previously been subjected to unrelated experimental procedures. Moreover, we did not evaluate the influence of the mouse sex on the results. All living animals were maintained in a specific-pathogen-free (SPF) animal facility. This facility was approved and monitored by the Institutional Animal Care and Use Committee (IACUC) at Academia Sinica, ensuring the ethical treatment of animals in the study.

Study animal tissue collection

Regarding the procedure of collecting animal tissues, mice were first

deeply anesthetized using 20 mg/mL Avertin (2,2,2-Tribromoethanol, Sigma), with the dosage determined according to their body weight. Once the mice were confirmed to be fully anesthetized, cardiac perfusion with cold phosphate-buffered saline (PBS) was carried out to remove any remaining blood. The tissues were then carefully collected and placed in Trizol (Thermo Scientific) to enable RNA extraction. Subsequently, perfusion was performed with freshly prepared 4% paraformaldehyde (PFA) in PBS to fix the tissues in preparation for immunostaining or *in situ* hybridization. The entire spinal cord was dissected, treated with sucrose for cryoprotection, and embedded in FSC 22 frozen section media (Leica). Following previously established protocols, the spinal cord was cut into 20-25 μ m-thick cryostat sections to facilitate further analysis [35]. Overall, these steps were carried out meticulously to ensure tissue integrity and quality preservation, thereby enabling accurate and reliable examination of the samples.

Mouse ESC culture and MN differentiation

In this study, we employed a well-established method for culturing and

differentiating embryonic stem cells (ESCs) into MNs [54]. On the seventh day of the differentiation process, cells were treated with trypsin and subsequently collected for fluorescence-activated cell sorting (FACS). This sorting procedure allowed us to obtain two distinct types of neurons, those expressing green fluorescent protein (GFP^{ON}) and those not expressing green fluorescent protein (GFP^{OFF}). These distinct populations were then subjected to small RNA-sequencing (RNA-seq) analysis as required for the study. It is crucial to emphasize that all cell lines utilized in this research underwent routine mycoplasma testing to ensure the accuracy and reliability of the experimental results, maintaining the study's scientific integrity.

Human ESC/iPSC culture and differentiation

Blood samples were obtained from two type I SMA patients and healthy volunteers, following their informed consent and approval by the respective Institutional Review Boards (IRBs) KMHIRB-20140087, KMHIRB-SV(II)-20150016, and AS-IRB01-15046. These samples were then reprogrammed into induced pluripotent stem cells (iPSCs)

using previously established methods [55]. Both embryonic stem cells (ESCs) and iPSCs were cultured on Vitronectin-coated dishes using Essential 8 medium (Thermo Fisher Scientific A1517001).

The direct differentiation of ESCs and iPSCs into spinal motor neurons (MNs) followed a previously described protocol [56]. Briefly, cells were dissociated into single cells using Accutase (A1110501, Thermo Fisher Scientific) and resuspended in a differentiation medium to form embryoid bodies (EBs). This medium was composed of Advanced DMEM (12634010, Thermo Fisher Scientific): Neurobasal medium (21103-049, Thermo Fisher Scientific) 1:1, supplemented with 1% N2 supplement (17512048, Thermo Fisher Scientific), 2% B27 supplement (17504044, Thermo Fisher Scientific), 2 mM L-Glutamine (25030081, Thermo Fisher Scientific), 50 U/mL penicillin-streptomycin (15070063, Thermo Fisher Scientific).

The process of early neuralization involved dual SMAD inhibition, followed by caudalization and ventralization induced by retinoic acid (Sigma-Aldrich R2625-100MG) and a smoothened agonist (Millipore 566650-5), respectively. To promote the transition from neural progenitor

cells to post-mitotic MNs, a gamma-secretase inhibitor (Millipore 565784-19) was added. On day 16 of differentiation, the EBs were dissociated and plated on poly-L-lysine (Sigma-Aldrich P4707) and Laminin (Thermo Fisher Scientific 23017-015) coated plates. The isolated MNs were cultured in a differentiation medium containing Y-27632 (Calbiochem 688000), BDNF (Peprotech 450-02), GDNF (Peprotech 450-51), and L-ascorbic acid for an additional two weeks. If needed, cells were treated with trypsin and collected for FACS on day seven to obtain GFP^{ON} and GFP^{OFF} neurons for small RNA-seq analysis. To ensure the accuracy and reliability of the experimental results, all cell lines underwent routine mycoplasma testing.

microRNA *in situ* hybridization and miRNA scope assay

All experimental procedures were carried out using diethylpyrocarbonate (DEPC)-treated water or PBS for washing steps and reagent preparation. For *in situ* hybridization, spinal cord cryosections were initially treated with 10 µg/mL proteinase K (Invitrogen), followed by acetylation in acetic anhydride/triethanolamine and fixation using 4% PFA. Sections

were then pre-hybridized in hybridization solution, consisting of various components, at room temperature for 2-4 hours before being hybridized with each miRNA probe overnight at 55°C. After post-hybridization washes in 2 X SSC and 0.2 X SSC at 55°C, in situ hybridization signals were detected using the NBT/BCIP (Roche) system, following the manufacturer's instructions. Upon completion of color development, slides underwent immunostaining as outlined below. The slides were then mounted in Aqua-Poly/Mount and examined using a Zeiss LSM 780 confocal microscope. 5' FITC-labeled LNA probes for miR-17-3p, miR-27a-3p, and miR-34a-5p were purchased from Exiqon. To detect miR-34c-5p, spinal cord samples were dissected, fixed with 4% PFA, and processed using miRNAscope™ technology (Advanced Cell Diagnostics) in accordance with the manufacturer's guidelines [35,57]. A customized probe was used to detect mmu-miR-34c-5p. These procedures ensured the accurate and reliable detection of miRNAs in spinal cord samples. By mounting the slides in Aqua-Poly/Mount and analyzing them with a confocal microscope, precise examination and evaluation of the miRNA expression patterns within the tissue samples were made

possible.

RNA isolation from CSF of SMA patients

In accordance with the manufacturer's guidelines, total RNA was extracted from cerebrospinal fluid (CSF) using a miRNeasy Serum/Plasma Advanced Kit (Catalog No.: 217204, Qiagen). The process involved a series of steps, such as sample preparation, binding of the RNA to a silica-based membrane, washing to remove contaminants, and ultimately, eluting the purified RNA in 30 µl of nuclease-free water.

RNA isolation and qRT-PCR

Total RNA was isolated from the collected samples using the Quick-RNA MiniPrep kit (Zymo Research), ensuring a high-quality RNA yield. For the analysis of miRNA expression, miRNA-specific primers from TaqMan MicroRNA Assays (Life Technology) were utilized to reverse-transcribe 100-200 ng of total RNA from each sample. The assays employed included miR-17-5p (Assay ID: 002308), miR-27a-3p (Assay ID: 000408), miR-34a-5p (Assay ID: 000426), miR-218-5p (Assay ID:

000521), miR-34b-5p (Assay ID: 002617), and miR-34c-5p (Assay ID: 000428).

Endogenous internal controls were used for normalization purposes. Ubiquitous miR-16 (Assay ID: 000391) was employed for mouse samples, while small nucleolar RNA RNU48 (Assay ID: 001006) was used for human samples. The exogenous spike-in normalization control for CSF samples was cel-miR-39 miRNA (Assay ID: 000200). Each quantitative real-time PCR was conducted in duplicate for every sample, with a minimum of three independent experimental samples. This approach ensured accurate and reliable miRNA expression analysis, allowing for precise evaluation of the miRNA profiles in the samples.

RNA-sequencing analysis

For the small RNA-seq analysis, raw reads were preprocessed using the adapter trimmer EARRINGS [58] and aligned with the custom NTA aligner Tailor (reference: mm10) [59]. Tailor was configured with a minimum sequence alignment length of 18 nucleotides and a maximum hit occurrence of up to 10 positions. Following alignment, each hit was

annotated using information from various genomic databases: GenCode (version 27) [60] for gene names and types, miRbase (version 22) [61] for pri-miRNA and pre-miRNA classification, and Repeat-Masker (RMSK) [62] to mask repeat regions in the genomes. Since each read could have multiple annotations, a hierarchy was established to resolve potential conflicts, with higher-order annotations overriding lower-ranked ones. The annotation hierarchy was set as follows: miRNA > RMSK > others.

Data normalization was necessary for comparison as datasets were collected and analyzed from different labs, experimental conditions, and designs. Two normalization approaches were applied: correction according to reads per million (RPM) and quantile normalization. RPM correction addresses sequencing depth bias, while quantile normalization balances data distributions across samples. Before implementing quantile normalization, reads with RPM values below five were removed as they likely represented insignificant or sequencing errors. Additionally, during the early stages of analyzing some samples, reads aligned to miR-10a constituted up to 90% of all reads, heavily

biasing RPM calculations and quantile normalization. To mitigate such artifacts, miRNAs with expression levels (in RPM) above the top 10% and below the bottom 10% were masked during normalization, preventing outliers from affecting the reliability of downstream analyses. Bulk RNA-seq was carried out on an Illumina HiSeq 2500 sequencing system, as previously described [57]. This comprehensive approach ensured accurate and reliable analysis of small RNA-seq data, enabling a robust comparison of samples from various sources and conditions.

Immunostaining

We carried out immunostaining following previously established methods, utilizing a range of commercially available primary antibodies [35,57]. These primary antibodies included guinea pig polyclonal anti-Isl1/2 (a gift from Thomas Jessell Laboratory, 1:1000 dilution), guinea pig anti-Hb9 (a gift from Dr. H. Wichterle, 1:1000 dilution), mouse monoclonal anti-NANOG (MABD24, Millipore, 1:500 dilution), rabbit polyclonal anti-OCT3/4 (SC-5279, Santa Cruz, 1:1000 dilution), rabbit monoclonal anti-ChAT (ZRB1012, Millipore, 1:100 dilution), goat

polyclonal anti-ChAT (AB144P, Millipore, 1:100 dilution), mouse monoclonal anti-Neurofilament H, Nonphosphorylated (SMI32) (801701 (clone SMI-32P), BioLegend, 1:1000 dilution), goat polyclonal anti-Isl1 (GT15051, Neuromics, 1:1000 dilution), and rabbit polyclonal anti-Laminin (L9393, Millipore, 1:100 dilution). Alexa488-, Cy3-, and Cy5-conjugated secondary antibodies were acquired from either Invitrogen or Jackson ImmunoResearch and used at a 1:1000 dilution. Images were captured with a Zeiss LSM710 or LSM780 confocal microscope.

For whole-mount staining of muscle neuromuscular junctions (NMJs), freshly dissected muscles were first fixed in 4% PFA for 2 hours, then washed overnight with PBS. The samples were permeabilized and blocked in 5% bovine serum albumin (BSA) in 1% Triton X-100/PBS at 4°C overnight [35]. Next, antibodies against neurofilament NF-M (2H3, Developmental Studies Hybridoma Bank, 1:100 dilution), a synaptic vesicle protein 2 (SV2, Developmental Studies Hybridoma Bank, 1:100 dilution), and α -bungarotoxin (BTX, B13422, Alexa fluor 555 conjugates, Thermo Fisher Scientific, 1:500 dilution) were added to the blocking

buffer and incubated at 4°C for 2 days. Following multiple PBS washes, muscle tissues were incubated overnight at 4°C with secondary antibodies. The muscles were then carefully separated, flattened, and mounted on slides before imaging.

Predicted MiR-34/449 target genes and gene ontology analysis

We employed the online database TargetScan (Release 7.1 or 7.2, available at http://www.targetscan.org/mmu_72) to identify potential target genes that are regulated by the MiR34/449 family. To further refine the selected candidates, we conducted gene ontology analysis using the Database for Annotation, Visualization, and Integrated Discovery (DAVID) [63]. In our previous study, we presented functional clustering annotations derived from DAVID, which were expressed in terms of gene enrichment. By using these comprehensive bioinformatics tools, we aimed to understand better the functional associations and roles of the target genes regulated by the MiR34/449 family [64].

scAAV9-MiR34a preparation and injection

A 700-bp mouse DNA fragment containing *Mir34a* was subcloned from the pENTR/D-TOPO-*Mir34a* plasmid [53] and inserted into the scAAV9-CMV plasmid. The resulting scAAV9-MiR34a construct was transfected into mouse MiR34a-KO ESCs to verify its expression before being packaged by the AAV Core Facility at Academia Sinica. For neonatal intravenous administration, a fresh solution of scAAV9 was prepared in sterile PBS with 0.3% Fast Green FCF (Sigma-Aldrich). At postnatal day 0, mouse pups were briefly anesthetized on ice for 1 minute. Under microscopy, 10^{10} viral genomes of scAAV9 in a 30 μ L solution were then injected into the temporal vein using a 30G needle (BD Ultra-Fine II). Injections were deemed successful if the pup instantly turned blue. After the procedure, injected pups were allowed to recover on a heating pad before returning to their home cage.

Statistical analysis

The finding results were displayed as the mean \pm standard deviation (SD), with each experiment conducted at least three times to ensure consistency, unless stated otherwise. GraphPad Prism 6.0 (GraphPad Software) was

utilized for statistical analysis. For multiple group comparisons, one-way or two-way analysis of variance (ANOVA) with Tukey's multiple comparisons test was employed, as indicated in the figure legends. The Student's t-test was used to compare two groups, and a p-value less than 0.05 was deemed significant. Spearman's correlation coefficient was applied to assess associations between variables. To prevent overfitting, individual linear models were fitted using baseline CSF miRNA and pNfH levels to predict HINE-2 score improvements on Day 482, considering the limited number of subjects. Individual models were evaluated using the F-test, and raw p-values from these tests were corrected with the Benjamini-Hochberg method, setting a false discovery rate threshold at 5%.

Data Availability Statement

All RNA-seq data have been deposited in the Gene Expression Omnibus database: GSE228244.

VI. Results

Serum miRNA profiling to identify candidate biomarkers

To quantitatively profile miRNAs, we performed TaqMan Low-Density miRNA Array from the serum of five healthy individuals and SMA patients (2 type III, 2 type II, and 1 type I), respectively (Figure 1A). We targeted to detection of more than 800 human-annotated miRNAs with the TaqMan probe. We then focused on miRNAs detected in all samples ($C_q < 35$). We applied a hierarchical clustering approach on the first four SMA patients and controls to differentiate miRNA profiling data between SMA and controls. Both hierarchical clustering and principle component analysis (using the first two principal components) showed a vague separation of SMA patients from controls. Furthermore, the wide-spreading diversity of control samples just presented a significant categorization of disease versus healthy based only on serum miRNA profile (Figure 1B). Nonetheless, we found that the disease identity of SMA was nosily distinguishable from the global serum miRNA profiling approach. Therefore, we subsequently checked if a subset of serum miRNAs differ according to disease status and thus are more informative

in telling disease from normal. We performed differential express analysis with R package limma to identify disease-relevant serum miRNAs. With the addition of two more samples (five SMA patients and controls, respectively), we uncovered five miRNAs (*miR-190*, *miR-21**, *miR-638*, *miR-642*, and *miR-661*) that were significantly differentially detected after correction for multiple comparisons (Figure 1C). However, the differential expression was still inconsistent among samples (Figure 1D).

Identification of miRNAs as candidate biomarkers through spinal MNs

Although SMA primarily manifests postnatally, growing evidence suggests that MN death and gene dysregulation can also occur during the embryonic stage [54,57,65,66]. Moreover, recent research indicates that the SMA pathomechanism affects motor neurons (MNs) and involves multiple interneurons (INs) within the spinal cord. Such a pathological link leads to disrupted sensory-motor circuitry, contributing to MN degeneration (Figure S1) [53,67,68]. Since early molecular dysregulation can result in postnatal neuronal loss and a decline in motor function, this

period offers a critical window for potential therapeutic intervention. (Figure S1) [69,70]. In order to better understand the molecular pathogenesis of SMA during the early stages of the disease, researchers have proposed that an authentic and reliable biomarker would need to meet two specific criteria. Firstly, it must consistently decline throughout the MN degeneration along with SMA disease progression. Secondly, such an authentic biomarker would need to be directly involved in the pathomechanisms of SMA. In an effort to identify potential biomarkers that meet these criteria, researchers have turned their attention to miRNAs particularly enriched in spinal cord. Given that the global profiling of miRNA from serum from individuals provides only limited information, we alternatively aimed to pursue candidate miRNAs that can express more specifically in spinal MNs during embryonic and adult stages. To circumvent this issue, we first looked at miRNAs in both MNs and INs using an embryonic stem cell (ESC) line expressing an MN transgenic reporter called Hb9::GFP [54]. Our previous study demonstrated that Hb9::GFP^{ON} cells are primarily enriched in Isl1/2 and Chat, while Hb9::GFP^{OFF} cells under the Shh^{low} condition are mainly

characterized by the expression of *Lhx1/5*, *Brn3a*, and *Gad1/2* [57]. After being sorted by fluorescence-activated cell sorting (FACS), the Hb9::GFP^{ON} embryonic MNs and Hb9::GFP^{OFF} embryonic INs were subjected to small RNA-seq (Figures 2A and 2B) (see details in Materials and Methods; Gene Expression Omnibus database: GSE228244).

Subsequently, we conducted a cross-referenced comparison between the embryonic spinal miRNAs we had identified and a public database of postnatal spinal neuronal miRNAs [67]. Through this analysis, we discovered a total of 187 miRNA candidates that were present in both datasets, implicating that they may be involved in the early stages of SMA pathology (Figure 2C). Among these potential miRNAs, MiR17, 23, 24, 27, 34, 125, and 181 were chosen for further assessments after reviewing references on candidates demonstrating miRNA functions in the spinal cord (Figures 2C and S2) [35,36,53,68,69]. To differentiate between the mouse gene and the mature form of miRNA, we used '*Mir34*' to represent the gene and '*MiR34*' to represent the mature miRNA throughout this study. Additionally, we applied one MN-enriched expressed miRNA (i.e., MiR218), and two previously identified

SMA-related biomarkers (i.e., MiR133 and MiR206) to assess in parallel their possible roles in SMA [70-72]. Finally, we performed *in situ* hybridization to validate the expression of our candidate spinal miRNAs *in vivo*. The results confirmed that MiR17a, 27a, and 34a were highly expressed in the ventral horn of mouse spinal cord sections on postnatal day 5 (P5) (Figure 2D).

Early dysregulation of MiR34 among SMA patient iPSC-differentiated MNs

We reprogrammed peripheral blood obtained from two SMA patients into induced pluripotent stem cells (iPSCs) to model type I SMA and assess whether our candidate spinal miRNAs reflect human pathology (Figure S3A). Reprogrammed iPSCs were maintained as ESC-like colonies in culture with or without a mouse embryonic fibroblast feeder layer (Figure S3B). We conducted various quality control assays and used an iPSC line derived from a type I SMA patient, which exhibited pluripotency markers NANOG and OCT3/4 (Figure S3C) and showed no abnormalities in the karyotype (Figure S3D). Western blotting confirmed that levels of SMN

proteins were drastically reduced in these two type I SMA ESC/iPSC lines compared to control iPSCs (Figure S3E). These findings suggested that two stable type I SMA patient-derived iPSC lines could thus be used for subsequent experiments.

The human spinal cord MNs were differentiated from iPSCs reprogrammed from two healthy controls and two patients with type I SMA, respectively, to investigate the dysregulation pattern of candidate miRNAs (Figures 3A and S3F) [35,56]. After two weeks, ~ 80% of the cells expressed ISL1 and SMI32, two generic markers representing human MNs (Figure 3B). Following the formation of embryoid body (EB)-derived colonies, long-term MN culture was established at day 11 by dissociation [35]. We defined the "critical window" MN development by identifying a significant decrement in the number of MNs, which could be evaluated by quantifying the ratio of MN expressing ISL1/2⁺/SMI32⁺ immunohistochemistry staining [73]. Our results were consistent with an earlier study [74], as we observed a significant reduction in the number of type I SMA MN lines compared to the healthy control groups when normalized against the total number of neurons at 6

weeks from the start of directed differentiation (Figure 3C).

In order to determine whether our candidate miRNAs are affected during and after a critical window of MN development, we assessed their expression levels in long-term spinal neuron cultures at weeks 6 (within the critical window) and week 8 (after the critical window). Of note, MiR34a was the only miRNA to exhibit significant downregulation within the critical window (Figure 3D). On the other hand, MiR24, MiR27a, MiR34a, MiR125b, and MiR133a/b showed significant downregulation in SMA-MN long-term cultures after the critical window, while MiR206 was undetectable and therefore excluded from further analysis (Figure 3E). These findings extracted from our human iPSC model of SMA show that MiR34a is a promising candidate significantly altered in the early stage of MN degeneration.

Validation of spinal miRNA dysregulation in SMN Δ 7 mice during the critical window for intervention

To discover potential biomarkers that can be informative for detecting the early critical window and thus guide SMA therapeutic plans, we

aimed to identify spinal miRNA candidates that showed dysregulation before the MN degeneration *in vivo*. To achieve this, we utilized homozygous mutant SMN Δ 7 mice that display motor deficiency and smaller body size in the first two weeks after birth compared to heterozygotic mice (Control) (Figure S4A) [75]. Based on our observation of a significant reduction in the MN population, as indicated by choline acetyltransferase (ChAT⁺) expression at P10 (Figures 4A and 4B), we defined P10 as the endpoint of the critical window in SMN Δ 7 mice. To further explore the dysregulation of spinal miRNAs during this period, we performed qPCR analysis to assess the expression levels of six candidate miRNAs, namely, MiR17, MiR27, MiR34a, MiR125b, MiR181a, and MiR218, at P10. MiR34a exhibited a consistent and substantial downregulation of these miRNAs in the spinal cord (Figure 4C), further validated by *in situ* hybridization (Figure 4D). Considering several factors brought out to the subsequent surveys, including (1) previous studies have highlighted roles for MiR34 in premotor INs and regulation of programmed cell death [53,76,77]; (2) MiR34 showed the most consistent declines across mouse and human SMA models (Figure 3

and Figure 4). Accordingly, we chose to focus on MiR34 expression levels in our subsequent study to investigate its role in the pathomechanism of SMA and clinical relevance used as a predictive biomarker.

The MiR34 family regulates motor-end plate function of neuromuscular junction

We regarded that an authentic biomarker for a disease would be more reliable and specific if it directly contributed to the disease's development. We, therefore, investigated whether the MiR34 family (MiR34a/bc) was involved in regulating the MN function. Notably, the MiR449 cluster also had the same function shared with the MiR34 family and contained the same seed sequence, making it difficult to distinguish their respective roles through genetic manipulations. To overcome this controversy, we have created a mouse model called the *Mir34/449* triple knockout (TKO) model. In this mice model, all six alleles were removed to avoid compensatory effects (*Mir34a*^{-/-}; *Mir34bc*^{-/-}; *Mir449*^{-/-} or *Mir34/449* TKO), providing us with a unique opportunity to examine the mechanisms in

MNs regulated by the MiR34/449 families [53].

Mir34/449 TKO mice experience two distinct periods of postnatal lethality, occurring during the second and fourth weeks, respectively, following birth. At P7, these TKO mice exhibited slowed growth compared to the littermate control (Ctrl) groups, as shown in Figure S4B. Previous research indicated that until P20, the number of MNs was comparable between the two groups [53]. While MN death accounts for a pathological hallmark of SMA, it has been suggested that functional deficits may be equally important. Evidence supporting this hypothesis includes studies where SMA mouse models were treated with Rho-associated kinase to disrupt P53 function, which resulted in prolonged life expectancy without rescuing MN loss [78,79]. On the other hand, even though the knockout of the *Bax* gene can rescue MN number and survival, growth delay persists, and only partial survival improvement is observed [80]. These findings led us to speculate that the deficiency of the SMN protein could disturb multiple parallel pathways, emphasizing the significance of investigating functional aspects beyond MN [6,81]. As a result, we conducted additional experiments to decipher

whether neuromuscular junctions (NMJ) morphology is affected in the *Mir34/449* TKO mice.

At first, we examined the presynaptic components, specifically MNs, in the NMJ motor end-plate using α -Bungarotoxin (α -BTX) labeling combined with immunostainings for neurofilaments (NF) and synaptic vesicle protein 2 (SV2) in intercostal muscles, which are one of the muscle types significantly affected by SMA in both patients and the SMN Δ 7 mouse model [82,83]. We analyzed wild type (WT), *Mir34a/449* double knockout (*Mir34a*^{-/-}; *Mir449*^{-/-} or *Mir34a/449* DKO), *Mir34/449* TKO (*Mir34a*^{-/-}; *Mir34bc*^{-/-}; *Mir449*^{-/-}), heterozygous (carrier) SMA and SMN Δ 7 mice. Surprisingly, both *Mir34/449* TKO and *Mir34a/449* DKO littermate mice showed significant presynaptic NF aggregation (Figure 5A, quantification in 5B). Subsequently, we examined the post-synaptic components by assessing the size of acetylcholine receptor (AChR) clusters in the intercostal muscles. Similar to SMN Δ 7 mice, the NMJ end-plates were smaller in *Mir34/449* TKO mice compared to DKO and WT groups (Figure 5C, quantification in 5D). We also evaluated myofiber growth impairment, another characteristic reported in SMN Δ 7 mice [82],

and observed a decrease in myofiber diameter of *Mir34/449* TKO mice, compared to *Mir34a/449* DKO littermates, in both the intercostal and gastrocnemius muscles (GA) at P7 (Figures 5E and 5G, quantification in 5F and 5H, respectively).

MiR34 family regulates synaptic formation pathways

To identify genes regulated by MiR34/449 in the spinal cord, we conducted RNA-seq analysis on the thoracic and lumbar segments of spinal cord tissues from P14 *Mir34/449* TKO mice age-matched WT mice, serving as the Control group (Figure 6A). These two segments were chosen as they are more affected in SMA mice models [75,84]. In the thoracic segments, we found 4021 upregulated and 2532 downregulated genes upon depletion of MiR34/449 (Figures 6B and 6D). On the other hand, 2265 upregulated and 1140 downregulated genes were identified in the lumbar segments (Figures 6C and 6E). Next, we aimed to identify target genes directly associated with MiR34/449, so we cross-referenced the upregulated genes against predicted MiR34/449 targets in the thoracic (Figure 6B) and lumbar (Figure 6C) regions, respectively. Gene ontology

(GO) analysis revealed several common terms in both segments, such as synapse-related and axon guidance terms (Figures 6B and 6C; Gene Expression Omnibus database: GSE228244), which are consistent with major dysregulated GO terms identified in previous studies on SMA mice [85-87]. Remarkably, we also observed that genes related to the NMJ were abnormally upregulated in the lumbar regions, which aligns with the phenotype observed in the *Mir34/449* TKO mice (Figures 5 and 6C). Therefore, it appears that the MiR34 family may regulate synapse formation and several core pathways that are disrupted in SMA during early postnatal stages.

Introduction of MiR34a in the neonatal period partially alleviates the severity of SMN Δ 7 mice

In the present study, we consistently observed declined levels of MiR34 in human and mouse models of SMA, which is known to affect the NMJs. To investigate whether restoring MiR34 levels could improve SMA symptoms, we gave newborn SMN Δ 7 mice a single dose of self-complementary adeno-associated vector serotype 9 (scAAV9)

containing MiR34a through intravenous injection on postnatal day 0 (P0). After administering the treatment, we evaluated the mice's motor function and conducted histological analyses at P7 (Figure 7A).

At P7, we confirmed that the MiR34a treatment increased the levels of MiR34a in the spinal cords of the treated SMA mice (Figure 7B). While the control group still showed altered NMJ characteristics of SMA in the intercostal muscles (including aggregated NF in pre-synaptic terminals of motor axons and smaller α -BTX-labeled end-plate area), the group treated with AAV-MiR34a showed significantly enlarged NMJ end-plates (Figures 7C-7E). Moreover, the treated group partially restored motor function as evidenced by the righting reflex test (Figures 7F and 7G). Notably, we also observed a significant negative correlation between the righting reflex index and end-plate area of SMA mice (Figure 7H), as well as between their righting reflex latency and spinal MiR34a levels (Figure 7I), suggesting that the improvement in motor function was due to the maintenance of NMJ integrity post-MiR34a treatment. These findings support the role of MiR34 in SMA pathology and suggest its potential as a therapeutic target for SMA. Further investigation is also

warranted to determine its predictive power in clinical settings.

MiR34 in the cerebrospinal fluid predicts the treatment response of nusinersen in type I SMA patients

Developing authentic biomarkers for SMA to predict disease progression and treatment response is crucial in light of existing programs for carrier and prenatal screening of SMN deficiency. To assess the effectiveness of a potential SMA biomarker, we examined longitudinal changes in MiR34 family expression levels in the CSF samples from seven type I SMA patients who underwent ASO (nusinersen) treatment at Kaohsiung Medical University Hospital. We determined the SMN2 copy number for each patient and recorded longitudinal assessments of their clinical features and motor function (Table 2). The average age of onset for SMA was 2.9 months, and the mean age for administering the first nusinersen dose was 8.6 months. Patients were given loading doses of nusinersen on days 0, 14, 28, and 64, followed by scheduled maintenance doses every four months (Figure 8A). We analyzed MiR34a, MiR34b, and MiR34c expression levels in the CSF at baseline (before the first nusinersen

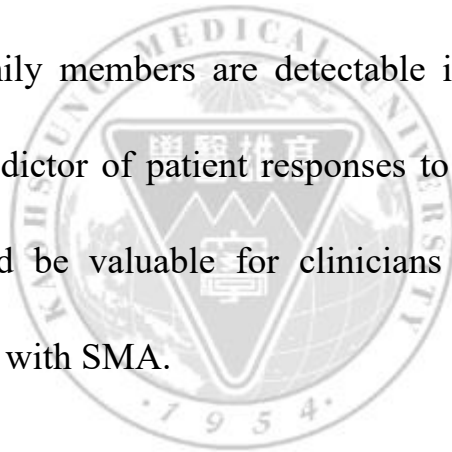
dosage) and on the day of the last loading dose (Day 64) (Figures 8B-8D). Levels of phosphorylated neurofilament heavy chain (pNfH) proteins in blood and CSF were proposed to reflect active axonal loss and may serve as a sensitive tool for the early detection of MN degeneration [88]. Thus, we used pNfH as a known biomarker to evaluate the predictive power of our baseline measurements in terms of motor function. We observed a decline in patient expression levels of MiR34a, MiR34b, and MiR34c upon nusinersen treatment except for patient SMA-2; Figures 8B-8D), similar to the decrement in pNfH levels (Figure 8E), which has been suggested to reflect early rescue of axonal pathology [89-91]. To determine the correlation between changes in biomarkers and motor function, we performed a Spearman's correlation analysis on the motor-function scale of the Hammersmith Infant Neurological Examination (HINE-2) against the expression levels of pNfH and the MiR34 family in CSF samples of type I SMA patients on Day 64, Day 183, and Day 482 after nusinersen treatment. As comparing baseline (day 0) and day 64 measurements may be affected by varied treatment responses among patients, we focused on relative changes in biomarkers

over time. We found no significant correlations during the loading phase of nusinersen therapy. However, at later treatment phases of Day 183 and Day 482, we observed negative correlations between relative changes in pNfH levels (Figures S5A-5C) and MiR34 family expression levels (Figures S5D-5I, especially MiR34b as shown in Figures 8F-8H) and improved HINE-2 scores.

Subsequently, the correlation between treatment responses and the levels of pNfH and the MiR34 family in the CSF led us to investigate whether their baseline measurements could predict treatment outcomes. We constructed individual linear regression models with HINE-2 changes on Day 482 as the dependent variable and pNfH/MiR34 expression at baseline as the independent variable. We performed an F-test to evaluate the predictive power of each model after multiple comparison corrections.

We found that baseline MiR34b in CSF was positively correlated with the HINE-2 score on Day 482 (Figure 8I), whereas pNfH did not reach the same significance. This finding echoes a recent study indicating that plasma pNfH could only predict motor function after treatment for over three years [92]. Altogether, our findings suggest that the MiR34 family is

an early and constant biomarker downregulated in human and rodent models of SMA. MiR34 may regulate the synaptogenesis pathway that maintains NMJ end-plate integrity. The loss of MiR34 function can impair NMJs and compromise muscle fiber size. At the same time, the delivery of MiR34a can mitigate SMA symptoms, which may provide additional evidence to support extra-MN involvements and SMN-independent pathways in SMA pathogenesis [93,94]. To our surprise, MiR34 family members are detectable in the CSF and could serve as an early predictor of patient responses to nusinersen treatment. These findings could be valuable for clinicians in guiding treatment decisions for patients with SMA.



VII. Discussion

While the versatile roles of miRNAs in regulating neural development have been well elaborated over the past two decades, the role of miRNAs in neurodegenerative diseases is just beginning to emerge. Regarding the pathogenic role of miRNA in MN degeneration, the first evidence showed that conditional deletion of the miRNA biogenesis enzyme Dicer in MNs using Olig2-Cre or ChAT-Cre results in MN degeneration resembles hallmark phenotypes of SMA and ALS [33,35,95]. This evidence suggests that miRNAs are pivotal regulators for MN diseases. In addition to the prominent role of SMN in regulating RNA processing, recent studies have suggested an association between SMN and RBP (RNA-binding protein), potentially participating in miRNA biogenesis. Mechanically, SMN could engage with the formation of miRNA–RBP or miRNAs (ribonucleoproteins harboring miRNAs) complexes and likely regulate miRNA biogenesis and metabolism. On the other hand, deficiency of SMN may further affect the biogenesis of miRNAs or miRNPs formation [96], attributed to MN degeneration. Recently, we have proposed underlying pathomechanisms that SMN-associated RBPs

might be involved in miRNA production and metabolism, including facilitating recruitment of Drosha to specific miRNAs, binding to components of the Drosha and Dicer complexes, or acting as regulators to RISC complex [36,45]. As a result, the dysregulation in forming the SMN-RBP complex, associated with SMN deficiency in the context of SMA pathology, could potentially disrupt the proper biogenesis of miRNAs and the splicing process of pre-mRNA molecules. Indeed, specific miRNAs have been proposed to be altered by SMA, a disease known to manifest as early as during the prenatal stage [81].

Herein we summarize the present study's research flow and main findings. At first, we hypothesize that the difference in candidate miRNAs might be reflected in human serum. However, our preliminary serum profiling data showed that serum miRNAs carry insufficient information to tell the difference between disease and healthy individuals in the context of SMA. Serum miRNA dysregulations are very noisy. Indeed, a previous study also found a poor correlation between serum candidate miRNA level and the clinical motor function of SMA patients

[37]. We reason that this inconsistency is probably due to gender, age, metabolism factors, etc. A better way to uncover bona fide miRNA markers might be through spinal cord MN-enriched miRNAs. Therefore, we tried to circumvent this limitation by profiling miRNA from ESC-derived MNs, the primary cells directly affected by SMA pathological background. Among the several miRNAs potentially participating in MN development in the spinal cord, we identified the MiR34 family downregulated in the early stages of SMA in both murine model and human iPSC-derived MNs. By utilizing the *Mir34/449* TKO mice, we resolved the functional redundancy among MiR34 family members and found that MiR34 family plays a role in maintaining the integrity of axonal end-plate. We suggested that the declined level of MiR34 in spinal MNs could result from SMN deficiency. Subsequently, several major dysregulated pathways were identified in *Mir34/449* TKO and SMA model mice, as well as in human iPSC models. Overexpression of MiR34a via scAAV9 injection in SMN Δ 7 mice showed restoration of NMJ end-plate size and improvement of the motor function. Data from a longitudinal study of CSF samples and motor development in our treated

type I SMA patients suggests that baseline levels of MiR34b in CSF might serve as a potential predictor for treatment outcome after one and a half years of nusinersen therapy. Furthermore, a negative correlation between CSF-circulating MiR34 and motor function measurements was observed in type I SMA patients receiving nusinersen treatment. Altogether, we propose that MiR34b and its associated MiR34 family members might represent promising biomarkers to predict treatment response in SMA patients and further reflect the post-treatment improvement in a real-time manner, given they demonstrate an ability to maintain the axonal end-plates of MNs that are negatively affected early in SMA pathogenesis [97].

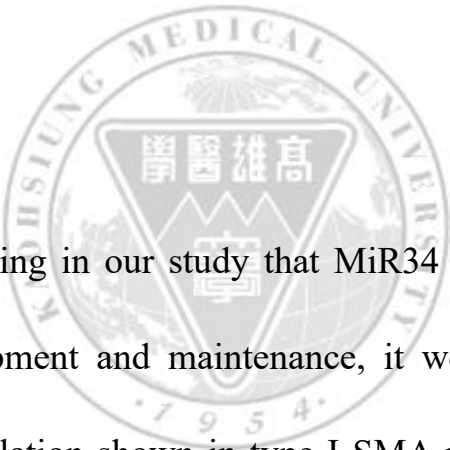
It is intriguing to reveal the pathomechanism link between MiR34 family and SMA. Recently, it was demonstrated that MiR34 contributes to the maintenance of postnatal IN numbers to regulate sensory-motor circuitry in the spinal cord [53]. Previous studies have also shown that alteration of sensory perception and motor output attributes to MN death in the early stage of SMA pathogenesis [98]. Indeed, sensory-motor circuit

dysfunction characterized by increased input impedance, impaired synaptic efficacy, and hyperexcitability has been reported to precede MN death in different SMA mouse models. [84,99-101]. In the present and our previous studies [53], we found that miR-34/449 TKO mice at postnatal stage manifest several SMA pathology hallmarks, including (1) aberrant sensory-motor circuit, (2) axon swelling, (3) compromised NMJ morphology, and (4) reduced myofiber size. However, we did not detect an obvious change in *Smn* expression in our *Mir34/449* TKO mice across all three spinal segments based on our RNAseq results. Additionally, *Smn* is not an in silico-predicted target of MiR-34/449 (both 5p and 3p). Accordingly, though *Mir34/449* TKO mice exhibited SMA phenotypes to certain degrees, the MiR34/449 family does not appear to regulate *Smn* expression directly. This scenario concurs with our RNAseq results showing that *Smn* expression is not compromised in the *Mir34/449* KO spinal cords. How SMN regulates the MiR34 family to participate in pathomechanism in SMA might need future studies to address this issue.

Previous studies showed that, in SMA mouse models, there is variable

resistance or vulnerability of MN degeneration, from medial to lateral and cranial-caudal in different spinal segments (i.e., T9 and L1) [84,102]. However, given the difficulty of obtaining postnatal *Mir34/449* TKO mice (50% of the TKO mice die before P14), we could only apply entire thoracic and lumbar segments to perform RNAseq on the *Mir34/449* TKO mice. Therefore, our approach might have overlooked some altered MiR34/449-mediated genes involved in SMA pathogenesis. Profiling through an approach of single-cell RNSseq among specifically vulnerable spinal segments might help to identify the full spectrum of altered gene expression regulated by MiR34 family and further to decipher their links to SMA pathology. *Mir34/449* TKO alters the expression of genes involved in axon guidance and synaptogenesis (Figure 5), so we cannot exclude the possibility that the MiR34 family could contribute to SMA pathology via sensory-motor circuit dysfunction and indirectly cause motor end-plate dysfunction. In addition, we did not observe any reduction in MN numbers in the *Mir34/449* TKO mice [53], nor did we see an increase in MN numbers in the AAV-MiR34a overexpression mice. This outcome is likely because the major role of MiR34 is to control synapse

function and integrity in the NMJs, an observation reflected in a study of *Drosophila* [103]. Nevertheless, our neuropathological findings from *Mir34/449* TKO mice indicate that synaptic defects might manifest at multiple levels of the spinal sensory-motor and peripheral neuromuscular circuitry, which has also been observed early in an SMA mouse model [100]. Thus, the multifaceted and versatile roles of the MiR34 family in spinal neurons might enhance its representation in the CSF, rendering detection less noisy.



Given the initial finding in our study that MiR34 family play a pivotal role in NMJ development and maintenance, it would be intriguing to know their downregulation shown in type I SMA patients after efficient nusinersen treatment. We believe that the MiR34 family functions as positive regulators of MN synapse formation, based on the findings: (1) *Mir34* family-KO mice display compromised NMJ morphology (Figure 5), and (2) AAV9-mediated *Mir34a* overexpression in the *SMA Δ 7* mouse model increased end-plate area and enhanced motor skills (Figure 7). Therefore, our interpretation of the negative correlation between MiR34

expression in the CSF and better treatment efficiency is that the normal physiological functions of the MiR34 family are to support robust NMJ physiological functions. Strikingly, a recent study showed that injection of a scAAV9 vector containing *miR-23a* into the later-onset phenotype SMA mouse model (*Smn*^{2B/-}) could increase MN size, endplate area of NMJ, and finally, survival time [104]. The detailed mechanisms underlying how *miR-23a*-mediated target pathways lead to SMA pathology have yet to be characterized. However, these findings suggest that a specific cohort of miRNAs might cause the vulnerability to NMJ of SMA, and identification of those miRNA culprits and their targets could provide a new treatment strategy for SMA. Indeed, several models have been postulated to explain how miRNAs in CSF can act as biomarkers for neurodegenerative diseases. First, it is known MNs degenerating progressively due to SMN deficiency. If the release of miRNAs is secondary to MN necrosis, MiR34 in the CSF will gradually increase in SMA patients as a reflection of progressively degenerating MNs. Therefore, our results revealed a negative correlation between the trend of MiR34 family levels in CSF and the improvement of motor function in

SMA patients positively responding to nusinersen treatment, which seems to corroborate this proposed model. Notably, a previously proposed biomarker of miRNA with positive role in maintaining MN function also showed downregulated levels in CSF of patients [105]. On the other hand, it is known miRNAs can excrete through selective and active exocytosis [43]. Thus, in SMA, selective package of MiR34 family members could be enhanced due to deficiency of SMN protein and consequently released from the affected MNs. These two models might explain our findings that the declined level of MiR34 family in the SMA iPSC-derived MNs and spinal cord of SMA mouse model, but increased level in CSF of untreated SMA patients. A future study aiming to investigate whether SMN protein interacts with the packing and/or releasing of MiR34 family member through a certain biomechanism might help to discover other potential miRNA working for SMA biomarkers.

Since identifying the causality between SMN loss and SMA phenotypes, several therapeutic approaches have focused on restoring SMN protein levels to rescue SMA, of which are generally termed “SMN-dependent

pathway.” Based on this proof-of-concept, three breakthrough therapies, either through the modulation of *SMN2* splicing: an antisense oligonucleotide (ASO) of nusinersen and a small molecular drug of risdiplam or the replacement with *SMN1*: onasemnogene abeparvovec, have been approved for the cure of SMA. Inspiringly, all of these agents have exhibited promising outcomes, especially in patients with severe type I undergone a newborn screen program. Other approaches, such as increasing SMN transcript levels, stabilizing SMN protein, and neuroprotective or cell therapies are currently undergoing development [106,107]. Although innovative SMA therapies continue to advance, emerging evidence shows that not all SMA patients responded equally to these therapies [26]. Thus, there is an urgent need to pursue more reliable markers to decipher the variable treatment response and to improve early detection and clinical management of patients with SMA [29,30]. Identifying authentic and reliable biomarkers can help improve the statistical power of clinical trials, reduce trial durations and costs, and facilitate clinical decision-making in a tailored way to adjust dosage and delivery interval to optimize therapeutic success [26,47,106,108].

Especially in SMA patients who always present with widely diverse phenotypes and relatively slow disease courses, an authentic biomarker should reliably reflect the progression or treatment success at each time point in different unrelated cohorts [30].

Biomarkers utilized in SMA clinical studies include circulatory biomolecules, physiological, structural (imaging modalities), and clinical measurements. However, no general agreement has been reached on the most reliable one. Regarding the application in monitoring treatment response, the assessments on SMA patients have largely relied on physiological, structural, and clinical parameters, such as motor function, electrophysiological tests, and pulmonary function [26,29]. Although these indicators are applicable, they can be limited by assessor bias, intra-, and interrater variability, lacking sensitivity, and dependency on patients' collaboration. For example, the motor score tests, such as the modified Hammersmith functional motor scale (MHFMS), can be inappropriate for children under 30 months and may not be comparable to motor score tests is specifically designed for young infants [30,109]. Because the disease

progression in SMA is usually slow, clinical outcome measures may become more unreliable to detect significant improvements in motor function in 1-2 years of follow-up during a randomized clinical trial [110]. Especially during the critical period of the COVID-19 pandemic, the principle of eliminating physical contacts and evaluation time for these particularly COVID-vulnerable patients with SMA makes these clinical assessments seem less feasible [111]. However, several longitudinal studies on patients with SMA have highlighted an emerging role of circulating molecular biomarkers in tracking disease progression and response to treatment [112]. The characteristics of easy accessibility, high reproducibility, relative objectivity, and cost-effective render molecular biomarkers a feasible option of large benefit for SMA patients who are often fragile and immobile. The role of circulating biomarkers spans a spectrum from prognostication to predicting treatment response and monitoring the effects of therapeutic agents. Especially in the SMA condition, the most affected cell type and the primary target of SMN-restoring therapies are MNs, which are complex and rarely accessible for patient quantity measurement [113]. Therefore, identifying

a set of reliable circulating biomarkers from accessible biofluids might help stratify the variability among patients and further improve the knowledge of therapeutics in SMA [114,115].

To date, several potential circulating biomarkers have been investigated for their applicability to monitor therapeutic response in SMA human and/or animal models by detecting peripheral or central biofluids (Table S1). Among these, neurofilaments, especially phosphorylated forms with heavy chain (pNF-H), have emerged as a leading marker for disease progression and treatment response in SMA infants [90]. Recent studies further demonstrated that pNF-H in plasma and CSF of type I SMA patients increased significantly, and declined rapidly within 2 months after nusinersen treatment [90,116]. It implied that level changes of pNF-H after SMA therapies may reflect the early biochemical effects on axonal rescue that precede clinical improvements in motor performance. As the introduction of SMA newborn screen program makes more and more SMA patients able to be treated at much earlier time points, pNF-H may help to guide the timing to initiate treatment, especially for

presymptomatic SMA patients. However, there are still limitations of applying pNF-H as a biomarker to monitor disease progression or treatment response for SMA. The characteristics of pNF-H is highly neuronal specific, but it is not exclusively specific for MNs. Several neurodegenerative diseases other than motor neuron involvements, such as Charcot-Marie-Tooth disease, Parkinson's disease and Alzheimer's disease also show elevated levels of pNF-H [117]. Fluctuating plasma levels of pNF-H have been reported both in healthy individuals as well as in SMA patients. In healthy individuals, these fluctuating levels in their early life may reflect the neuronal physiological development associated with pruning process, such as programmed cell death, remodeling of polyneuronal muscle fiber innervation, or any combination of these [90]. With a half-life up to 8 months, the findings of changed NFs levels in peripheral blood specimens may only reflect CNS condition occurring weeks or months earlier [115]. In addition, NFs appear to be less successful as predictive and pharmacodynamics biomarkers for individuals with chronic forms of SMA. Compared to normal controls, neither the levels of NFs in serum nor in CSF changed in type 2 or 3

SMA patients after nusinersen treatment [118,119]. The changed levels of pNF-H have been proven to poorly correlate with motor function improvement in milder form SMA patients after nusinersen treatment [120,121]. The lack of pNF-H level changes in adult SMA patients may be related to the exhaustion of the MN pool during the progression of chronic disease [118]. In brief, evidence suggests that pNF-H might not be a perfect biomarker in predicting treatment response in adolescent or adult types of SMA, at any point throughout the disease course.

On the other hand, recently improved detection methods for circulating miRNAs in biofluids have provided greater sensitivity and precision, making miRNAs represent authentic biomarkers for different motor neuron diseases, including SMA [122-125]. Recent studies also show that changes miRNAs level in biofluids can reflect the response to ASO therapy among SMA patients with different phenotypes [72,126-128]. Here, we have shown that MiR34b in the CSF exhibits equivalent or a better ability to predict treatment responses to an ASO-based treatment when compared with pNfH. Our preliminary multivariate linear model

that simultaneously considers pNfH and the MiR34 family presented improved prediction accuracy compared to individual pNfH/MiR34b models. Although we cannot rule out a contribution of multivariate model over-fitting given our current sample size, improved model accuracy by enhancing sample size could indicate that pNfH and MiR34b are not redundant and that multiple weak predictors could form a stronger ensemble model. A strong predictive model could help determine if dose adjustment or a combinatorial approach is needed for SMA patients that are predicted to respond poorly to treatment. In this study, we used mouse ESC-derived MNs and INs as paradigms to search for potential miRNAs that are involved in SMA disease progression and that might serve as mechanistic biomarkers for predicting disease treatment outcomes. It remains to be tested if other miRNAs that are expressed in the adult spinal cord or some specific miRNAs that only exist in humans may also act as good candidates. It will be tantalizing to explore if the MiR34 family, together with other identified miRNA biomarkers such as MiR133/181/206 [37,38,72], as well as other yet-to-be-discovered candidates, could be pooled as an “SMA disease treatment prediction

biomarker panel” for clinical application in the real world.

We recognize that our study has certain limitations. In the following sections, we will discuss these limitations in detail and suggest possible future research directions to expand the scope of our study. This will help enhance our understanding of the role of MiR-34 in SMA. First, we found there was a lack of control group in this study making it hard to reliably assess nature change of MiR34 change in healthy and SMA patients without treatment. Although a significant correlation was observed between the motor function improvements and baseline MiR34b levels , as well as during the treatment course in nusinersen-treated SMA patients, in the treated SMA patients, lacking the data of control groups, such as normal individuals and/or untreated SMA patients, makes it difficult to assess the nature changes of MiR-34 level. For example, fluctuating pNF-H levels have been reported in healthy individuals and untreated SMA patients, suggesting the confounding effect of neuronal physiological development [90,118]. A methodological consideration for future studies is to include age-matched control cohort for every SMA

phenotype. In addition, it will be of interest to investigate the predictive power of miR34 in SMA patients treated by several curative agents other than ASO, including marketed onasemnogene abeparvovec and/or risdiplam. A recent study had been done to detect neurofilament levels of SMA patients treated by nusinersen and/or onasemnogene abeparvovec [129]. They concluded that neurofilaments cannot be used as the single marker to predict outcomes of either therapeutic agent. Again, these findings implied a panel of combined molecular biomarkers could be a resolution to enhance their validity and reliability [72].

Second, the statistic power of the present study is restricted by a small sample size and only selection of one phenotype of SMA (type I). An insufficient sample size proved a major limitation for our ability to assess the predictive power of the MiR34 family for ASO treatment outcomes. The functions of the MiR34/449 family are redundant in the context of SMA, as corroborated by the observation that SMA-like phenotypes are only manifested by *Mir34/449* TKO mice. We focused on MiR34a, given that its expression is more enriched in the spinal cord compared to

MiR34b and MiR34c [53], and it displayed the most consistent down-regulation across the different SMA models tested in this study. Therefore, we anticipated that MiR34a would serve as a better predictor of ASO treatment outcomes. Although we did observe that all MiR34 family members exhibited a similar downward trend in the CSF of SMA patients upon nusinersen treatment, our sample size limited our ability to address multicollinearity and identify which member is the most predictive. We admit that MiR34a is not a superior predictor in the cohort when compared to MiR34b/c but, considering the co-expressing nature of the family, all members carry very similar information. Besides, the limited number of patients in our longitudinal study made it impossible to retain a validation dataset for a prediction model. Thus, our model might be prone to overfitting, despite our best endeavors to limit the degrees of freedom. The lack of the MiR-34 data in types II and III SMA patients after nusinersen treatment makes it difficult to conclude its validity in treatment response in chronic form of SMA. As a previous study suggested that MiR-34 may have “second wave (fourth week)” of MN death in the *Mir34/449* TKO mice model [53], the relevant data from

chronic type SMA animal model and patients would be intriguing. Notably, a recent study showed that reintroduction of miR-23a through scAAV9 showed improvement of NMJ integrity and survival of *Smn2B^{-/-}* mice, a mice model exhibiting progressive motor neuron death during mid and late symptomatic stages of SMA disease progression [104]. Taken together, testing a larger cohort and including milder severities of SMA mice and patients will be required in future to determine if there is a significant difference in their predictive power.

Third, we failed to comprehensively analyze the interaction between MiR-34 and SMN. We did not investigate whether MiR34 could modify or interact with the SMN protein expression levels. A recent study reported that SMN transcript levels are not altered by their proposed SMA-related miRNAs [38], which is consistent with our transcriptomic study here in which *Smn* expression remained comparable between control and *Mir34/449* TKO mice. Additionally, *Smn* is not an in silico-predicted target of MiR-34/449 (both 5p and 3p). Accordingly, though *Mir34/449* TKO mice exhibited SMA phenotypes to certain

degrees, the MiR34/449 family does not appear to regulate Smn expression directly. This scenario is concordant with our RNAseq results showing that Smn expression is not compromised in the *Mir34/449* TKO spinal cords. Therefore, we speculate that deficiency of SMN protein might alter MiR34a expression, and the mechanistic link between SMN and the MiR34 family warrants further study. To better clarify a direct causal relationship of miR34 deregulation in SMA, we could evaluate the miR-34 levels after reintroducing SMN gene in the SMA human iPSC-derived spinal MNs. This could help us to determine if doing so upregulates MiR34a, which could help to clarify if MiR34a exerts a causative role in SMA. Furthermore, future experiments could also be designed to investigate whether SMN protein interacts with the molecular machinery that packs and secretes miRNAs. To better understand how MiR-34 is packed and secreted in different body fluids, future studies should compare the levels of MiR-34 in both serum and CSF samples. This is important because serum samples are more easily accessible in the human body, and analyzing both types of samples can provide more comprehensive information about MiR-34 acting as a predictive

biomarker.

Last but not the least, we have yet to identify the specific downstream targets upon which the MiR-34 family exert their effects. As it has been suggested that MNs in different segments of spinal cord might have different vulnerability to SMA pathology, manifesting a spatial and temporal differences (e.g., medial-to-lateral and cranial-caudal MN vulnerability). However, due to entire segments of thoracic and lumbar spinal cords used in our study, we may overlook some genes involved in MNs degenerations affected by MiR34/449. Therefore, using a single-cell RNAseq approach to identify the full spectrum of dysregulated genes mediated by MiR34 and establishing their functions and possible links to SMA according to specific vulnerable spinal segments via a single-cell RNAseq approach would be illuminating. Besides, it could be intriguing to identify the MiR34 targets responsible for disease phenotypes via gain-of-function and loss-of-function mechanisms (e.g., Delta/Notch signaling pathway experiments).

VIII. Conclusion

We proposed that the MiR34 family can act as a mechanistic biomarker of SMA and exert multifaceted functions in regulating both MNs and sensory-motor circuits in the spinal cord. The CSF levels of one family member of MiR34, especially MiR34b, at baseline and during nusinersen therapy are predictive and are correlated with motor function after treatment. Therefore, we propose that the MiR34 family represents a set of promising biomarkers to assess responses to SMN-restorative therapies. Future research involving a more extensive cohort of SMA patients with varying degrees of severity and control groups is needed to strengthen the reliability and validity of MiR34 as a biomarker for SMA. Additionally, examining MiR34 level changes in a more easily accessible biofluid, such as serum, and conducting studies with extended follow-up periods would be beneficial. Furthermore, assessing the predictive power of MiR34 for the other two FDA-approved SMA treatment agents could provide more valuable insights into its potential as a biomarker for SMA.

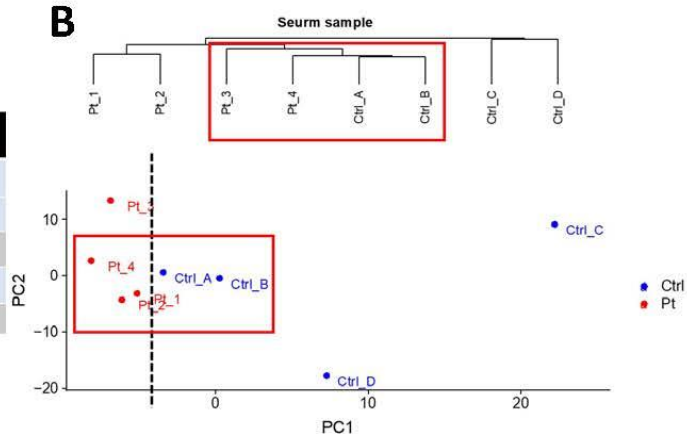
Figures and Tables



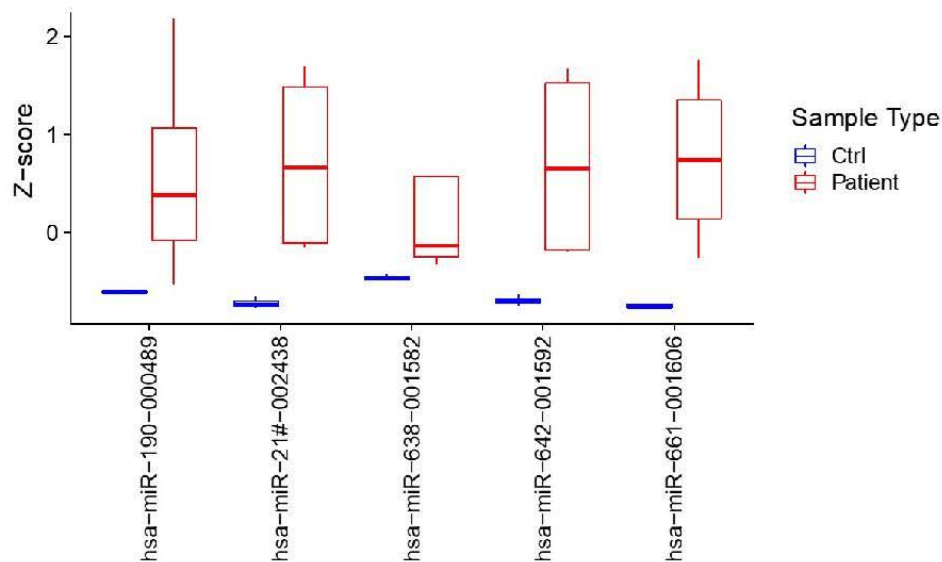
A

Patient No.	Age	SMA type	SMN1:SMN2
SMA-001	52 y/o	3	0:3
SMA-002	6 y/o	2	0:3
SMA-003	44 y/o	3	0:3
SMA-004	40 y/o	2	0:3
SMA-005	13 y/o	1	0:3

B



C



D

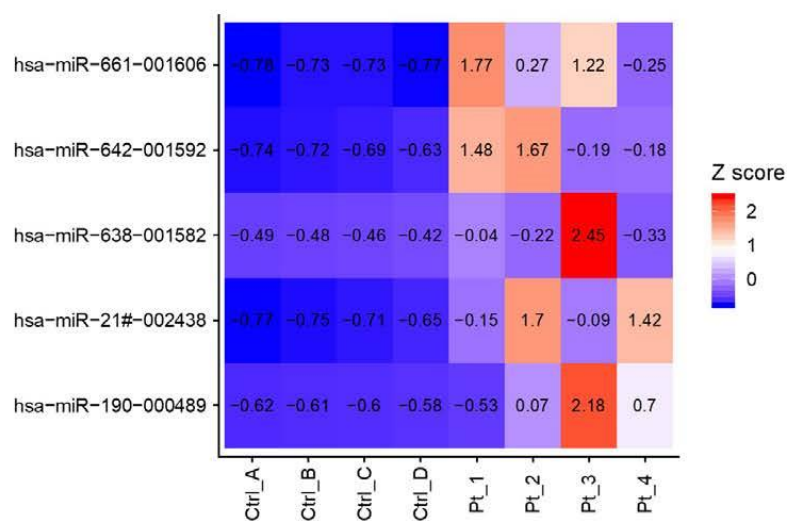


Figure 1. Profiling serum miRNAs to identify potential biomarkers for SMA

(A) Demographic data, genotype and clinical phenotypes of patients whose serum was analyzed. (B) Multidimensional scaling plot demonstrated the separation between the SMA and the control serum samples based on the miRNAs expression profile. The SMA samples are presented in red, and the controls are in blue. Global miRNA profiling of serum samples just presented vague, but insignificant, differences between of SMA patients and healthy individuals. (C) Five miRNAs (*miR-190*, *miR-21**, *miR-638*, *miR-642*, and *miR-661*) expressed differently after correction for multiple comparison. (D) Summary of the mapping of the reads for each sample. However, the differential expression of the profiled 5 candidate serum miRNAs showed no consistency among enrolled subjects.

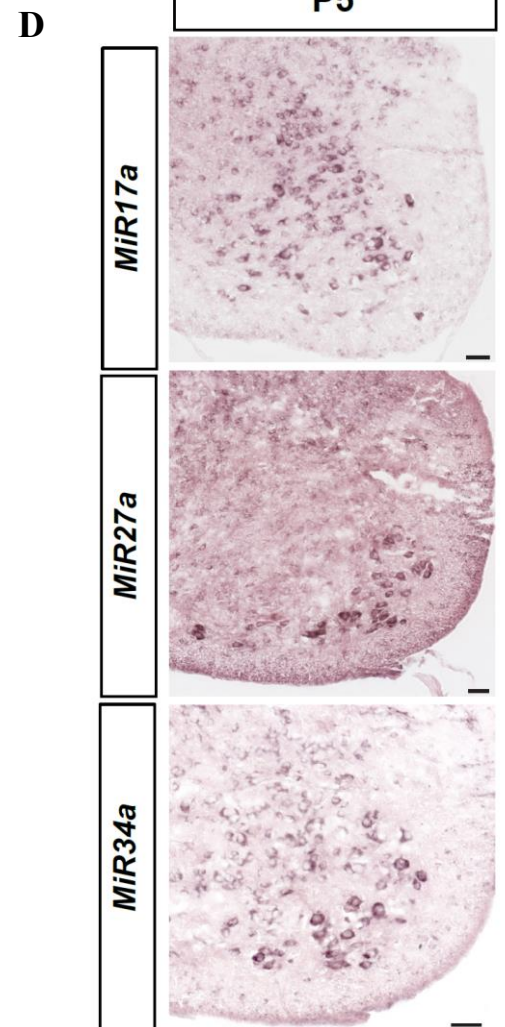
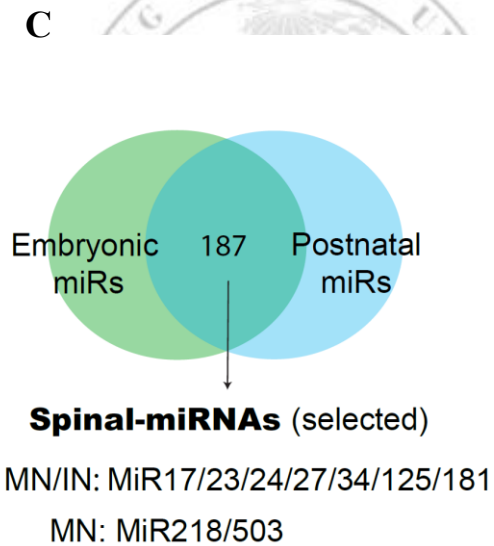
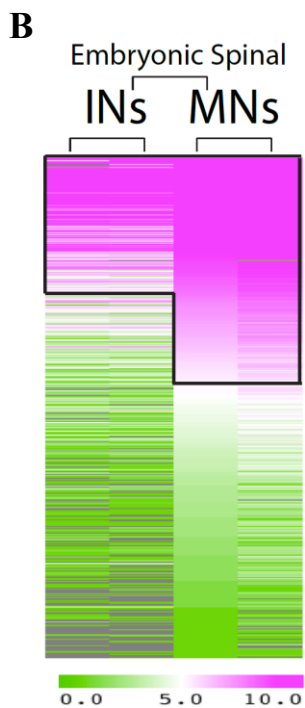
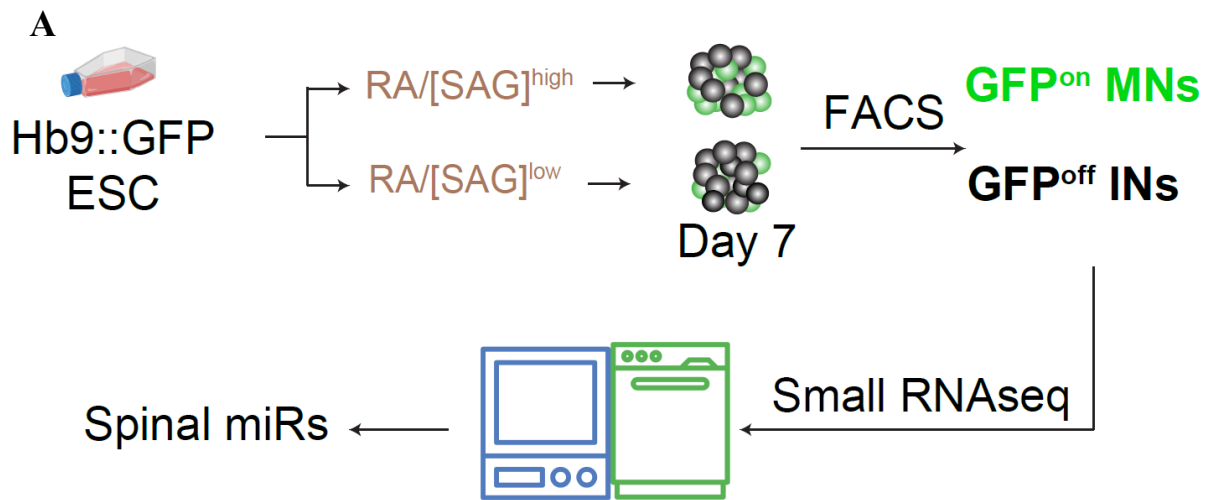
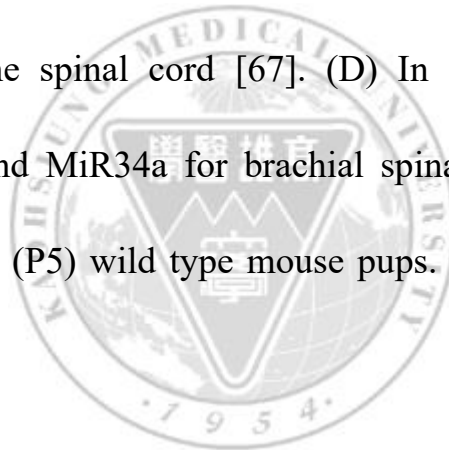


Figure 2. Identification of spinal miRNAs.

(A) Schematic illustration of the differentiation process from Hb9::GFP ESCs to spinal MNs and INs. RA: retinoic acid; SAG: Smoothed agonist; ESC: embryonic stem cell; MN: motor neuron; IN: interneuron. (B and C) Heatmaps (transcripts per million [TPM]) presenting miRNA abundances. miRNAs enriched in MNs and INs were selected for cross-referencing against postnatal expression patterns and those enriched in the spinal cord [67]. (D) In situ hybridizations of MiR17a, MiR27a, and MiR34a for brachial spinal cord sections taken from postnatal day 5 (P5) wild type mouse pups. Scale bar is 50 μ m in (D).



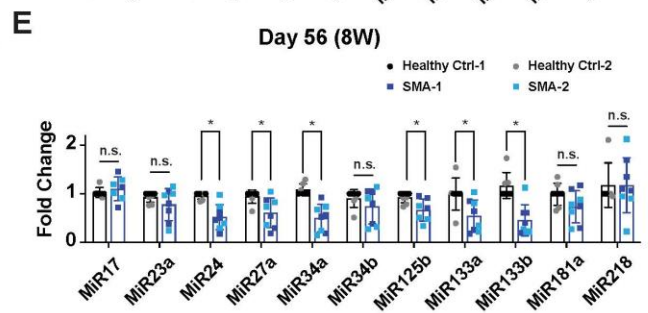
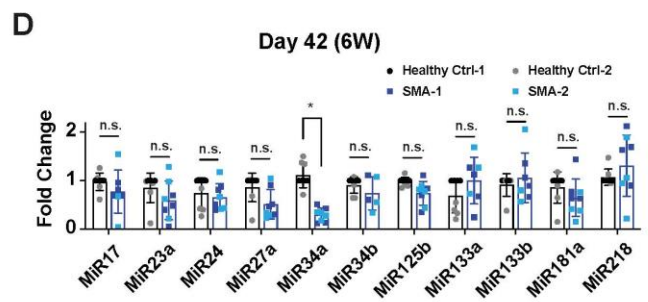
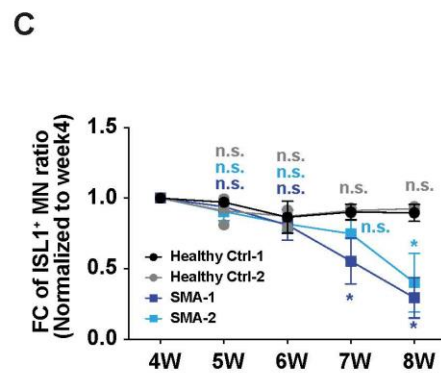
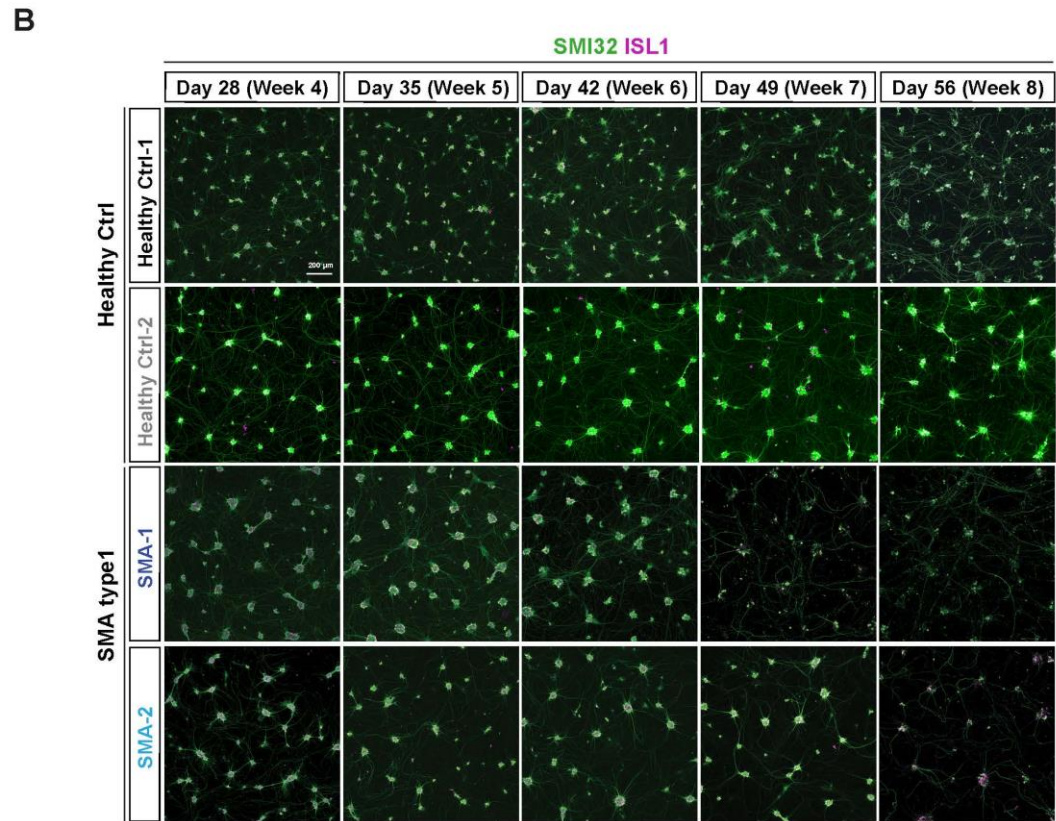
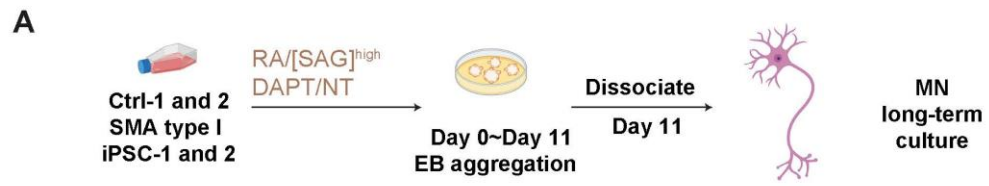


Figure 3. Dysregulated spinal miRNAs in SMA iPSC-derived MNs.

(A) Schematic illustration of the differentiation process from two type I SMA iPSCs to spinal MNs. iPSC: induced pluripotent stem cells; EB: embryoid bodies; MN: motor neurons. (B and C) MN survival in long-term MN cultures was assessed by quantifying the ISL1⁺/SMI32⁺ iPSC-derived MNs and determining the ratio to the day 4 population by immunostaining, which revealed a significant decline in SMA MNs after the 7th ~8th week (quantified in C, statistical analysis of each cell line compared to the ctrl-1 iPSC line). (D and E) Expression of spinal miRNAs in SMA MNs relative to ctrl-1 MN cultures at week 6 (6W, before MN degeneration) and week 8 (8W, after MN degeneration). We observed a notable decline in MiR34a levels prior to MN degeneration. Data are shown as mean \pm SD of fold-change (FC) relative to the ctrl-1 cell line. T. test by simple main effect analysis for Figure C (FC: fold-change; n.s.: not significant; error bars represent SD, n = 3~4 independent experiments; * p-value<0.05, by Student's t-test). Two tailed t test for (D and E); * denotes P< 0.05.

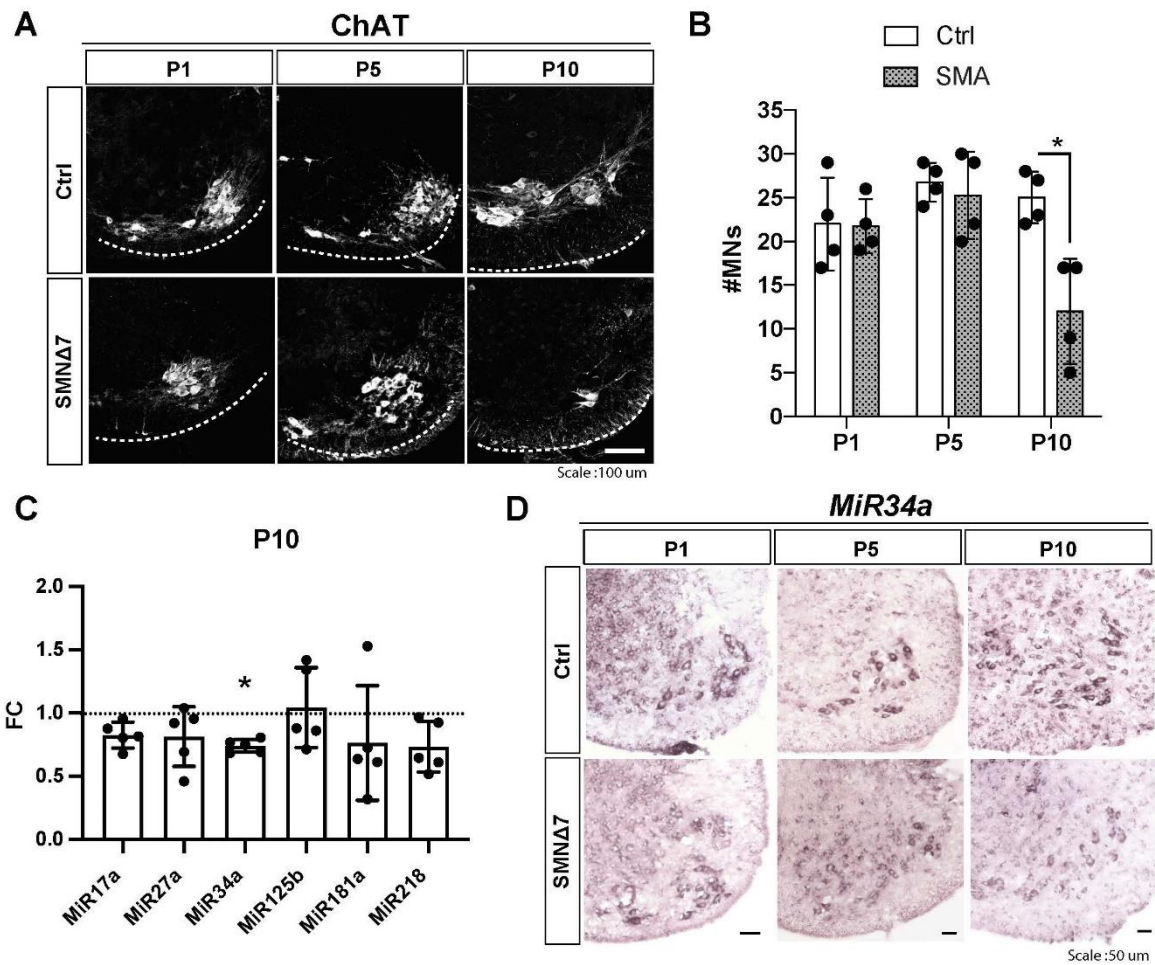


Figure 4. Dysregulated spinal miRNAs in SMNΔ7 mice.

(A) Immunostainings of spinal cord from P1, P5, and P10 SMNΔ7 mice reveals reduced ChAT⁺ MN signal at postnatal day 10 (P10). (B) Quantification of ChAT⁺ MN number in SMNΔ7 mouse spinal cord. (C) Expression of spinal miRNAs in P10 spinal cord of SMNΔ7 mice. Data are shown as fold-change (FC) relative to Ctrl mice. (D) *In situ* hybridization of MiR34a in P1, P5 and P10 ventral-half spinal cords.

Data are presented as mean \pm SD; * denotes $P < 0.05$; Scale bars represent 100 μm in (A) and 50 μm in (D).



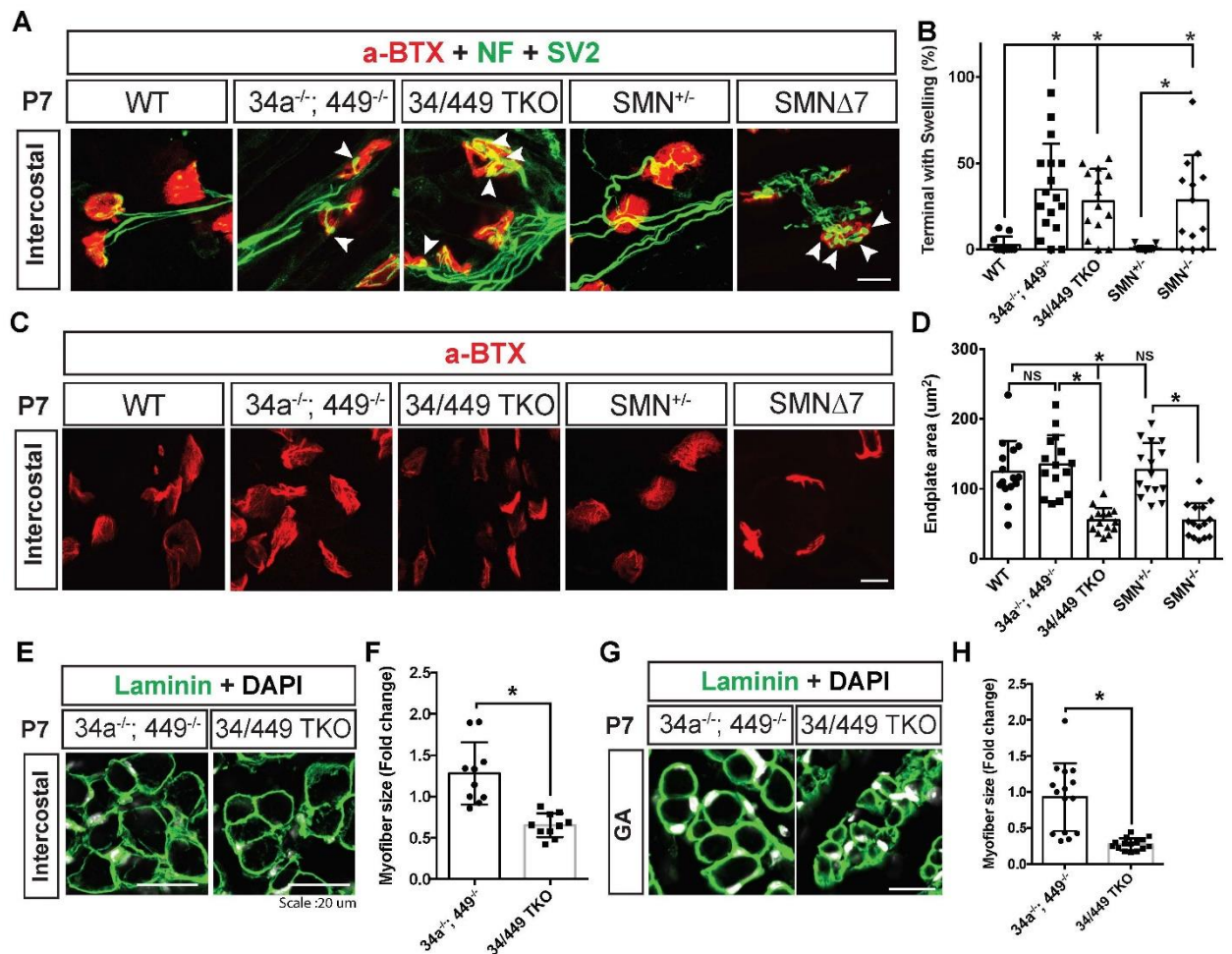


Figure 5. *Mir34/449* TKO mice display axon swelling and compromised NMJ end-plates.

(A) Immunostainings for NMJs in the intercostal muscles of *Mir34/449* TKO and SMNΔ7 mice using anti-NF and SV2 antibody (green) and α-BTX (red). Abnormal axonal swellings are indicated by arrowheads.

(B) Quantification (as percentage) of swollen axonal terminals from (A).

(C) Representative images of α-BTX-mediated labeling of AChR (red) in intercostal muscles from wild type (WT) and *Mir34/449* TKO mice at P7.

SMN Δ 7 and control (SMN^{+/-}) mice were analyzed in parallel to compare phenotypes. (D) Quantification of NMJ end-plate area from (C). (E and G) Immunostaining of laminin (green) in the intercostal (E) and gastrocnemius (GA) muscle (G) of P7 *Mir34/449* TKO mice and their *Mir34a*^{-/-}; *449*^{-/-} littermate control. Nuclei were labeled with DAPI (white). (F and H) Quantification of the myofiber size from intercostal (E) and GA (G) muscle immunostainings. Myofibers in the *Mir34/449* TKO muscle are smaller than for the Ctrl group. Scale bars represent 10 μ m in (A) and (C) and 20 μ m in (E) and (G). Data are presented as mean \pm SD; one-way ANOVA with Tukey's multiple comparisons test was performed in (B) and (D); Student t test was applied in (F) and (H). * denotes $P < 0.05$; "NS" denotes "not significant".

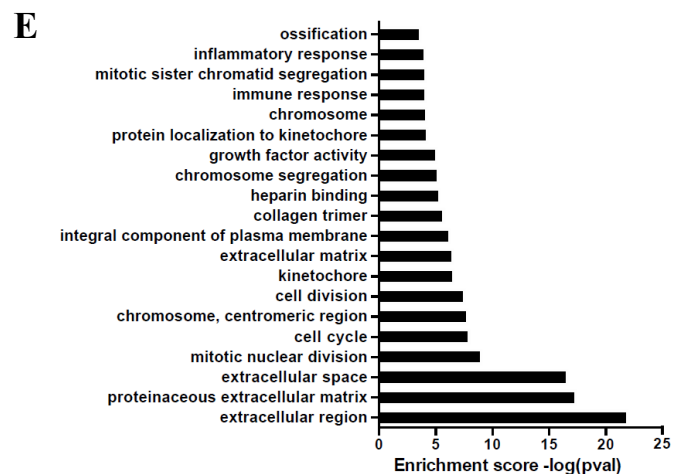
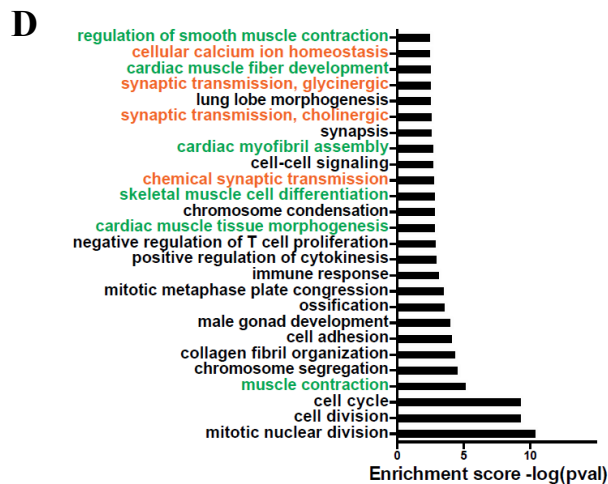
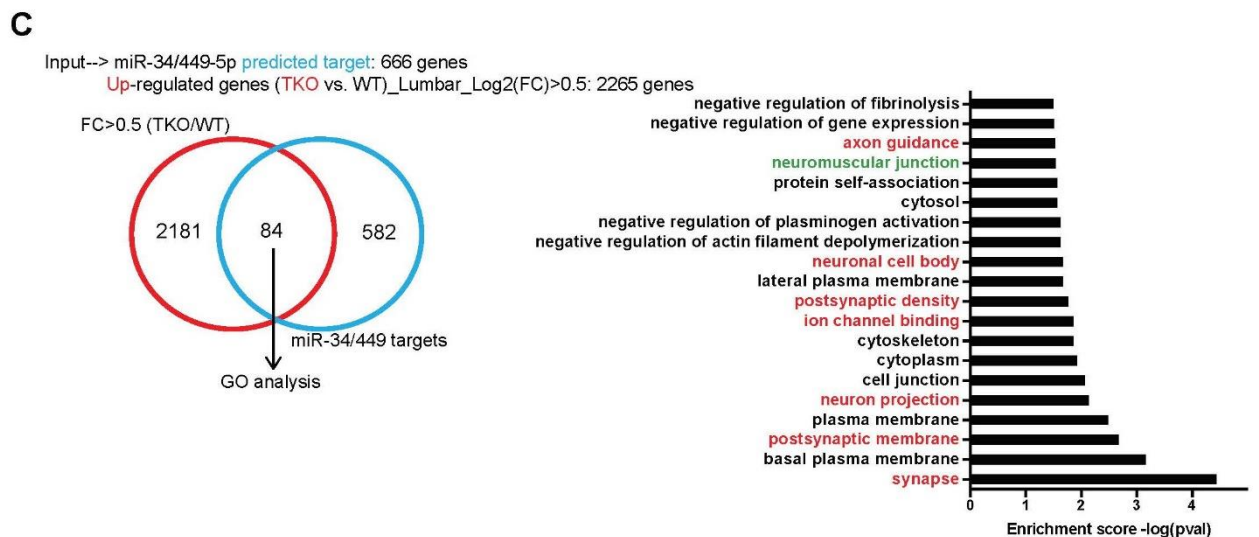
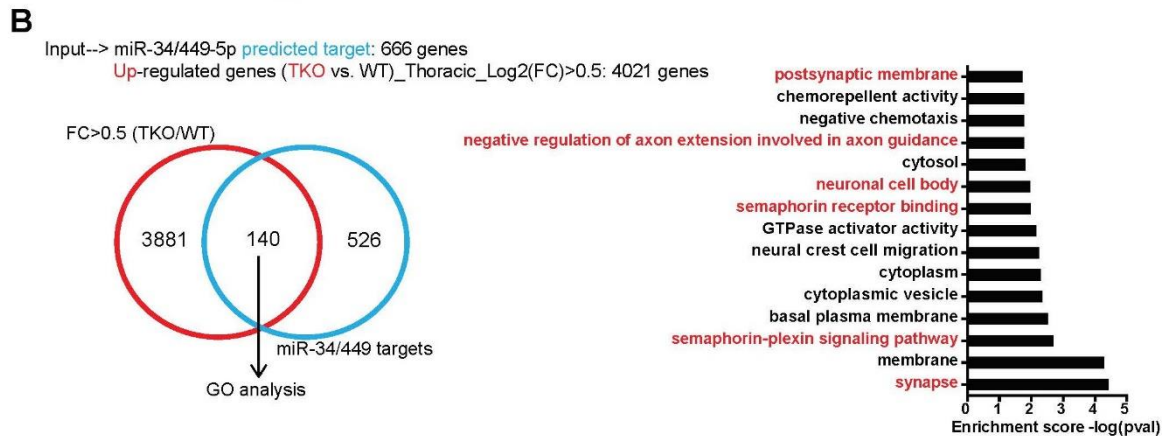
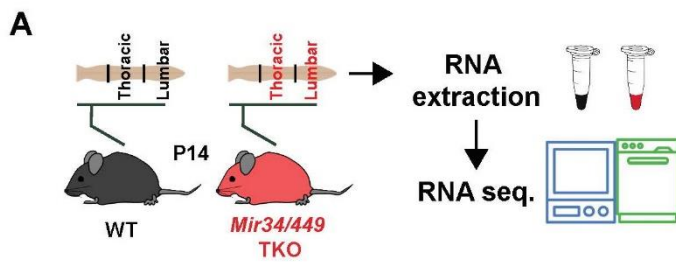


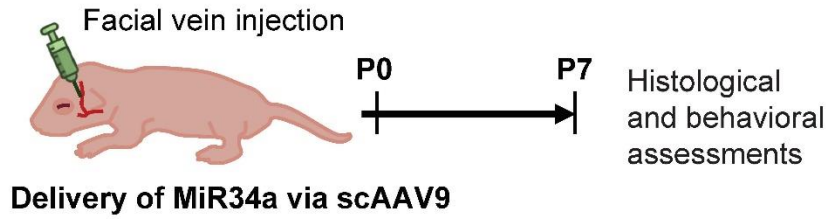
Figure 6. The MiR34 family regulates synapse formation pathways.

(A) Experimental strategy to perform RNA-seq on thoracic and lumbar segments from *Mir34/449* TKO and WT spinal cords at P14. (B and C) Strategy to identify potential MiR34/449 targets in *Mir34/449*-depleted spinal cord. The Venn diagram shows overlap of genes upregulated in the thoracic (4021 genes; B) or lumbar spinal cord (2265 genes; C), and the predicted MiR34/449 targets according to TargetScan (666 genes). Differentially expressed genes between *Mir34/449* TKO versus WT were filtered out according to the criteria of $p < 0.01$ and \log_2 fold-change > 0.5 . Intersecting genes from thoracic segment (n=140) as well as lumbar segment (n=84) are predicted to be *in vivo* targets dysregulated in the *Mir34/449* TKO spinal cord. Intersecting genes from left panel were subjected to gene ontology analysis in the right panel. Potential pathways related to the synaptogenesis and neuromuscular phenotypes are highlighted in red and green, respectively. (D&E) Downregulated genes from the thoracic spinal cord (n=2532; D) and lumbar spinal cord (n=1140; E) derived as in Figure 5A were subjected to GO analysis. Differentially expressed genes between *Mir34/449* TKO and WT mice

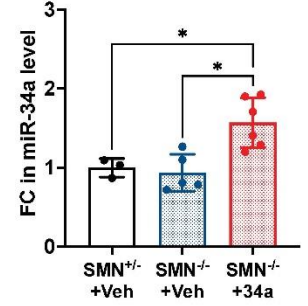
were filtered according to the criteria of $p < 0.01$ and \log_2 fold-change < -0.5 . Potential pathways related to muscle development and synaptic transmission phenotypes are highlighted in green and orange, respectively.



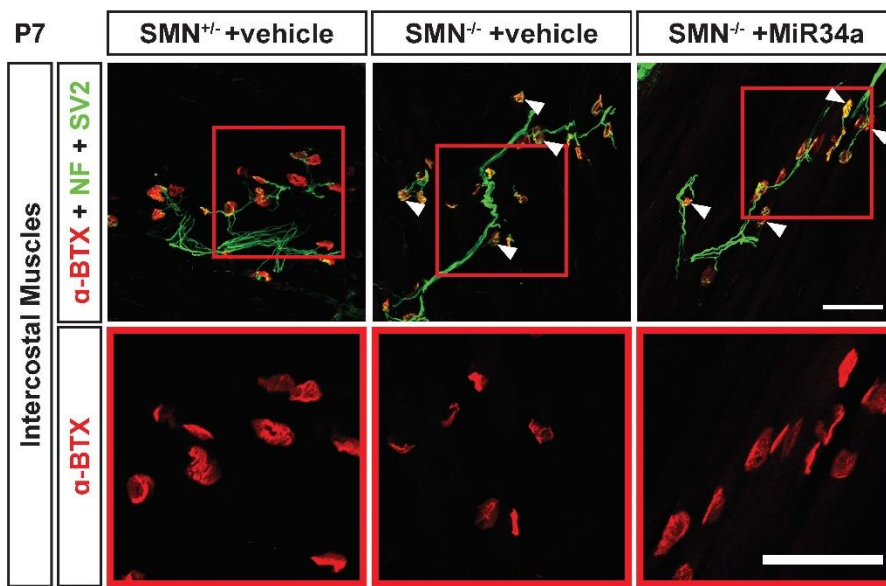
A



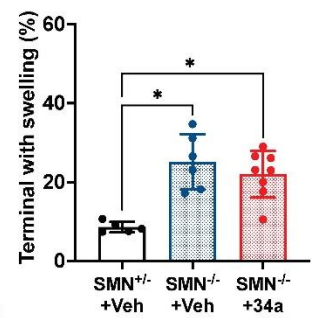
B



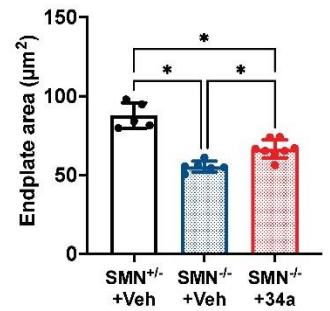
C



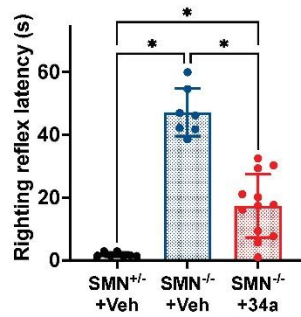
D



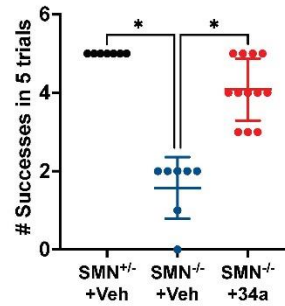
E



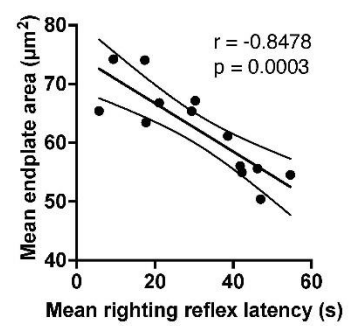
F



G



H



I

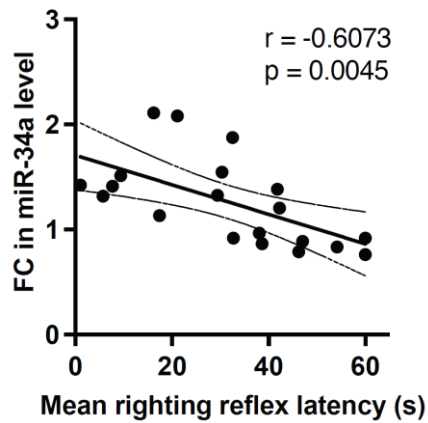
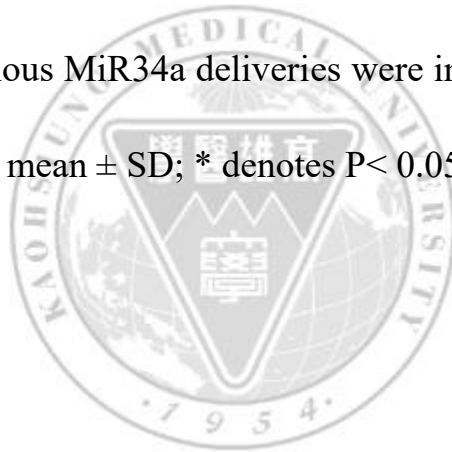


Figure 7. Neonatal delivery of MiR34a partially rescues the disease phenotype of SMN Δ 7 mice.

(A) Schematic illustration of the MiR34a overexpression experiments using the SMN Δ 7 mouse model. (B) Induction of MiR34a expression by scAAV9 vector in the spinal cord of SMN $^{-/-}$ mice was verified via qPCR. (C) Immunostaining for NMJs in the intercostal muscles was performed using anti-NF and SV2 antibody (green) and α -BTX (red). Arrowheads indicate swollen axonal terminals. Areas enclosed by the red rectangles have been enlarged to help visualize the size of motor end-plates. Quantitative analyses are presented in bar graphs for (D) the swollen axonal terminals and (E) the size of motor end-plates. Righting reflex latency (F) and success rate (G) were quantified as indexes of motor

function for mice at P7. (H) Pearson's correlation analysis was performed to evaluate the correlation coefficient (r) between righting reflex latency and end-plate area. (I) A significant negative correlation was observed between the righting reflex latency and spinal MiR34a levels of SMN Δ 7 mice. Pearson's correlation analysis were performed and coefficients (r) lower than -0.5 indicate a strong inverse correlation. All SMN Δ 7 mice (n=20) including those treated with vehicle, MiR34a, or with unsuccessful intravenous MiR34a deliveries were included in the analysis. Data are presented as mean \pm SD; * denotes $P < 0.05$; Scale bar: 50 μ m.



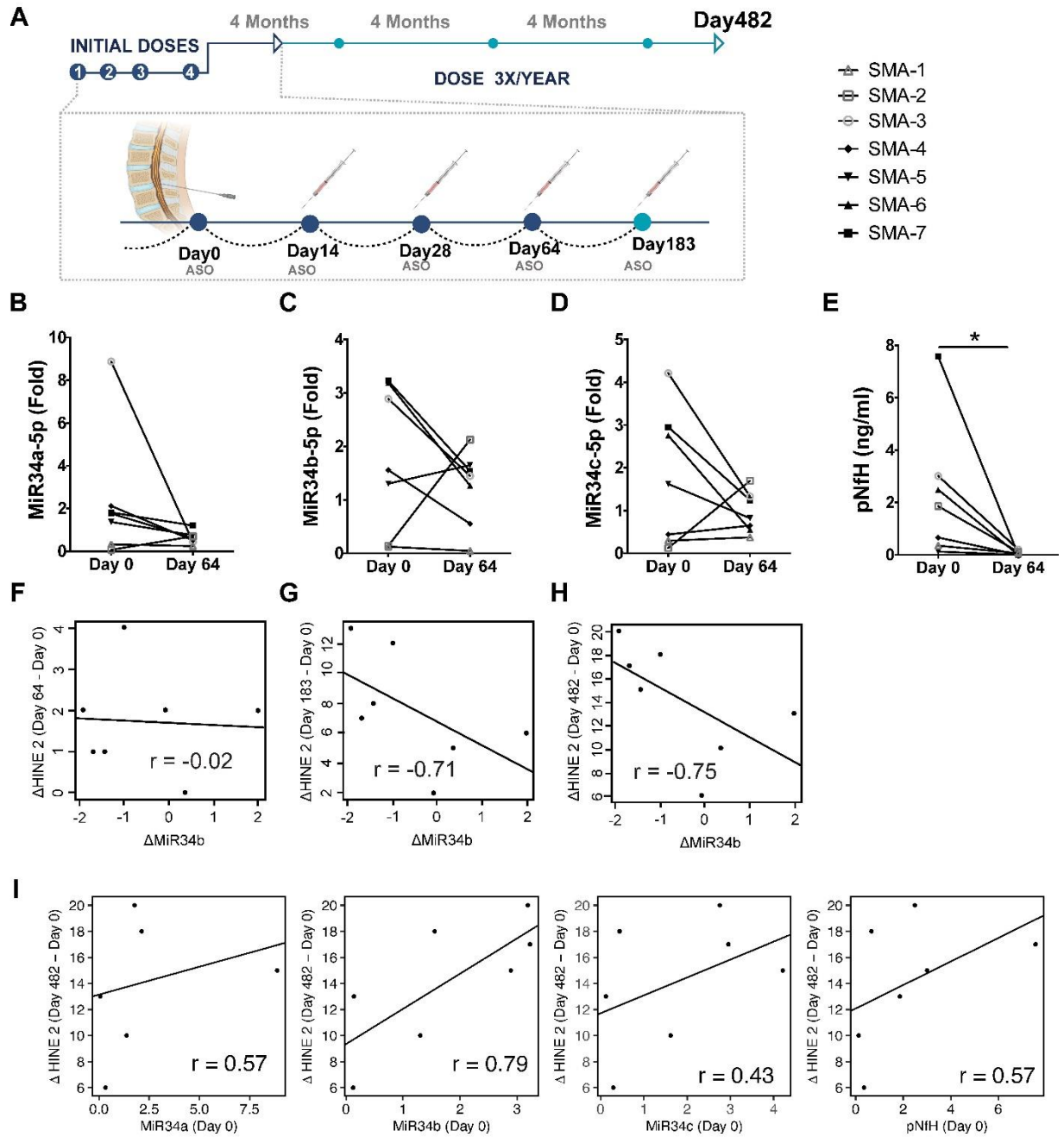


Figure 8. Trend for MiR34 reduction in type I SMA patients following nusinersen treatment.

(A) Schematic illustration of the treatment time-course for nusinersen (an ASO). (B-D) Expression of MiR34a (B), MiR34b (C), and MiR34c (D) in

the CSF of type I SMA patients after two months of nusinersen treatment.

(E) Levels of phosphorylated neurofilament heavy chain (pNfH) in the CSF of type I SMA patients before (Day 0) and after two months (Day 64) of nusinersen treatment. (F-H) Correlation between changing HINE-2 scores over the nusinersen treatment time-course and the change in MiR34b levels after two months (Day 64) of nusinersen treatment. Coefficients (r) lower than -0.5 indicate a strong inverse correlation. (I) Correlation between changing HINE-2 scores after 482 days of the nusinersen treatment and the basal expression level in CSF of the MiR34 family and pNfH before nusinersen treatment (day 0). Coefficients (r) higher than 0.5 indicate a strong correlation.

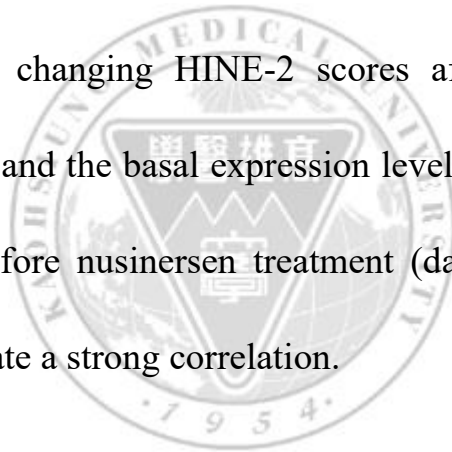


Table 1. List of primers for mouse genotyping

Gene name	Forward Primer	Reverse Primer
<i>miR-34a</i> WT	ATACCCTGGATCTCCAACAG	ACAAGACCCTCACCTGAATG
<i>miR-34a</i> KO	ATACCCTGGATCTCCAACAG	GCCATCCTGTTGAGGGACTA
<i>miR-34bc</i> WT	ATGACTTTACGGGGTTGACAG	AAATTCCTCCGACTGAGCCT
<i>miR-34bc</i> KO	ATGACTTTACGGGGTTGACAG	TTGCGGGAAGAAGGACTC
<i>miR-449</i> WT	GTTCCCCCAAGGTGAGTTTT	CCTGACACACCCACACTTCA
<i>miR-449</i> KO	GTTCCCCCAAGGTGAGTTTT	TGGAAACTTGGGCAAATACA
<i>mSmn</i> WT	CTCCGGGATATTGGGATTG	TTTCTTCTGGCTGTGCCTTT
<i>mSmn</i> KO	CTCCGGGATATTGGGATTG	GGTAACGCCAGGGTTTTCC

Table 2. Clinical features and motor function evaluations of SMA type I patients before and after nusinersen treatment

Patient	Gender	SMN2 Copy Number	Age at onset [m]	Age at first infusion [y]	HINE 2 score at baseline [Day 0]	HINE 2 score at D64 of treatment	HINE 2 score at D183 of treatment	HINE 2 score at D482 of treatment
1	F	3	3.4	2.21	2	4	4	8
2	F	2	3.8	0.41	0	2	6	13
3	M	2	1.4	0.33	0	1	8	15
4	M	3	4	0.7	2	6	14	20
5	F	3	4.6	1.14	3	3	8	13
6	F	2	2.1	0.27	0	2	13	20
7	M	2	0.7	0.1	0	1	7	17

X. References

1. Rochette, C.F.; Gilbert, N.; Simard, L.R. *SMN* gene duplication and the emergence of the *SMN2* gene occurred in distinct hominids: *SMN2* is unique to homo sapiens. *Hum Genet* **2001**, *108*, 255-266.
2. Lunn, M.R.; Wang, C.H. Spinal muscular atrophy. *Lancet* **2008**, *371*, 2120-2133.
3. Monani, U.R. Spinal muscular atrophy: A deficiency in a ubiquitous protein; a motor neuron-specific disease. *Neuron* **2005**, *48*, 885-896.
4. Burghes, A.H.; Beattie, C.E. Spinal muscular atrophy: Why do low levels of survival motor neuron protein make motor neurons sick? *Nat Rev Neurosci* **2009**, *10*, 597-609.
5. Singh, R.N.; Howell, M.D.; Ottesen, E.W.; Singh, N.N. Diverse role of survival motor neuron protein. *Biochim Biophys Acta Gene Regul Mech* **2017**, *1860*, 299-315.
6. Hamilton, G.; Gillingwater, T.H. Spinal muscular atrophy: Going beyond the motor neuron. *Trends Mol Med* **2013**, *19*, 40-50.
7. Tu, W.Y.; Simpson, J.E.; Highley, J.R.; Heath, P.R. Spinal muscular atrophy: Factors that modulate motor neurone vulnerability. *Neurobiology of disease* **2017**, *102*, 11-20.
8. Chaytow, H.; Faller, K.M.E.; Huang, Y.T.; Gillingwater, T.H. Spinal muscular atrophy: From approved therapies to future therapeutic targets for personalized medicine. *Cell Rep Med* **2021**, *2*, 100346.
9. Chen, T.H., Wang, C. H. Emerging innovative therapies of spinal muscular atrophy: Current knowledge and perspectives. In *Frontiers in clinical drug research - cns and neurological disorders*, Rahman, A.-u., Amtul, Z., Ed. Bentham Science Publisher: Sharjah, United Arab Emirates, **2020**, *8*, 1-34.
10. Finkel, R.S.; Mercuri, E.; Darras, B.T.; Connolly, A.M.; Kuntz, N.L.; Kirschner, J.; Chiriboga, C.A.; Saito, K.; Servais, L.; Tizzano, E., *et al.* Nusinersen versus sham control in infantile-onset spinal muscular atrophy. *N Engl J Med* **2017**, *377*, 1723-1732.
11. Mercuri, E.; Darras, B.T.; Chiriboga, C.A.; Day, J.W.; Campbell, C.; Connolly, A.M.; Iannaccone, S.T.; Kirschner, J.; Kuntz, N.L.; Saito, K., *et al.* Nusinersen versus sham control in later-onset spinal muscular atrophy. *N Engl J Med* **2018**, *378*, 625-635.
12. Hua, Y.; Sahashi, K.; Hung, G.; Rigo, F.; Passini, M.A.; Bennett, C.F.; Krainer, A.R. Antisense correction of *smn2* splicing in the cns rescues necrosis in a type iii sma mouse model. *Genes Dev* **2010**, *24*, 1634-1644.

13. Hua, Y.; Vickers, T.A.; Baker, B.F.; Bennett, C.F.; Krainer, A.R. Enhancement of smn2 exon 7 inclusion by antisense oligonucleotides targeting the exon. *PLoS Biol* **2007**, *5*, e73.
14. Foust, K.D.; Wang, X.; McGovern, V.L.; Braun, L.; Bevan, A.K.; Haidet, A.M.; Le, T.T.; Morales, P.R.; Rich, M.M.; Burghes, A.H., *et al.* Rescue of the spinal muscular atrophy phenotype in a mouse model by early postnatal delivery of SMN. *Nat Biotechnol* **2010**, *28*, 271-274.
15. Mendell, J.R.; Al-Zaidy, S.; Shell, R.; Arnold, W.D.; Rodino-Klapac, L.R.; Prior, T.W.; Lowes, L.; Alfano, L.; Berry, K.; Church, K., *et al.* Single-dose gene-replacement therapy for spinal muscular atrophy. *N Engl J Med* **2017**, *377*, 1713-1722.
16. Ratni, H.; Ebeling, M.; Baird, J.; Bendels, S.; Bylund, J.; Chen, K.S.; Denk, N.; Feng, Z.; Green, L.; Guerard, M., *et al.* Discovery of risdiplam, a selective survival of motor neuron-2 (smn2) gene splicing modifier for the treatment of spinal muscular atrophy (sma). *J Med Chem* **2018**, *61*, 6501-6517.
17. Baranello, G.; Darras, B.T.; Day, J.W.; Deconinck, N.; Klein, A.; Masson, R.; Mercuri, E.; Rose, K.; El-Khairi, M.; Gerber, M., *et al.* Risdiplam in type 1 spinal muscular atrophy. *N Engl J Med* **2021**, *384*, 915-923.
18. Kariya, S.; Obis, T.; Garone, C.; Akay, T.; Sera, F.; Iwata, S.; Homma, S.; Monani, U.R. Requirement of enhanced survival motoneuron protein imposed during neuromuscular junction maturation. *J Clin Invest* **2014**, *124*, 785-800.
19. Dangouloff, T.; Servais, L. Clinical evidence supporting early treatment of patients with spinal muscular atrophy: Current perspectives. *Ther Clin Risk Manag* **2019**, *15*, 1153-1161.
20. Aragon-Gawinska, K.; Daron, A.; Ulinici, A.; Vanden Brande, L.; Seferian, A.; Gidaro, T.; Scoto, M.; Deconinck, N.; Servais, L.; Group, S.M.-R.S. Sitting in patients with spinal muscular atrophy type 1 treated with nusinersen. *Dev Med Child Neurol* **2020**, *62*, 310-314.
21. Farooq, F.; Molina, F.A.; Hadwen, J.; MacKenzie, D.; Witherspoon, L.; Osmond, M.; Holcik, M.; MacKenzie, A. Prolactin increases smn expression and survival in a mouse model of severe spinal muscular atrophy via the stat5 pathway. *J Clin Invest* **2011**, *121*, 3042-3050.
22. Farooq, F.; Balabanian, S.; Liu, X.; Holcik, M.; MacKenzie, A. p38 Mitogen-activated protein kinase stabilizes SMN mRNA through RNA binding protein HuR. *Hum Mol Genet* **2009**, *18*, 4035-4045.

23. Hofmann, Y.; Lorson, C.L.; Stamm, S.; Androphy, E.J.; Wirth, B. Htra2-beta 1 stimulates an exonic splicing enhancer and can restore full-length SMN expression to survival motor neuron 2 (SMN2). *Proc Natl Acad Sci U S A* **2000**, *97*, 9618-9623.
24. d'Ydewalle, C.; Ramos, D.M.; Pyles, N.J.; Ng, S.Y.; Gorz, M.; Pilato, C.M.; Ling, K.; Kong, L.; Ward, A.J.; Rubin, L.L., *et al.* The Antisense Transcript SMN-AS1 Regulates SMN Expression and Is a Novel Therapeutic Target for Spinal Muscular Atrophy. *Neuron* **2017**, *93*, 66-79.
25. Wirth, B.; Karakaya, M.; Kye, M.J.; Mendoza-Ferreira, N. Twenty-five years of spinal muscular atrophy research: From phenotype to genotype to therapy, and what comes next. *Annu Rev Genomics Hum Genet* **2020**, *21*, 231-261.
26. Ramdas, S.; Servais, L. New treatments in spinal muscular atrophy: An overview of currently available data. *Expert Opin Pharmacother* **2020**, *21*, 307-315.
27. Baranello, G.; Gorni, K.; Daigl, M.; Kotzeva, A.; Evans, R.; Hawkins, N.; Scott, D.A.; Mahajan, A.; Muntoni, F.; Servais, L. Prognostic factors and treatment-effect modifiers in spinal muscular atrophy. *Clin Pharmacol Ther* **2021**, *110*, 1435-1454.
28. Navarrete-Opazo, A.; Garrison, S.; Waite, M. Molecular biomarkers for spinal muscular atrophy: A systematic review. *Neurol Clin Pract* **2021**, *11*, e524-e536.
29. Kariyawasam, D.S.T.; D'Silva, A.; Lin, C.; Ryan, M.M.; Farrar, M.A. Biomarkers and the development of a personalized medicine approach in spinal muscular atrophy. *Front Neurol* **2019**, *10*, 898.
30. Smeriglio, P.; Langard, P.; Querin, G.; Biferi, M.G. The identification of novel biomarkers is required to improve adult SMA patient stratification, diagnosis and treatment. *J Pers Med* **2020**, *10*, 75.
31. Ludwig, N.; Leidinger, P.; Becker, K.; Backes, C.; Fehlmann, T.; Pallasch, C.; Rheinheimer, S.; Meder, B.; Stahler, C.; Meese, E., *et al.* Distribution of mirna expression across human tissues. *Nucleic Acids Res* **2016**, *44*, 3865-3877.
32. Pelaez, N.; Carthew, R.W. Biological robustness and the role of micornas: A network perspective. *Curr Top Dev Biol* **2012**, *99*, 237-255.
33. Haramati, S.; Chapnik, E.; Sztainberg, Y.; Eilam, R.; Zwang, R.; Gershoni, N.; McGlinn, E.; Heiser, P.W.; Wills, A.M.; Wirguin, I., *et al.* Mirna malfunction causes spinal motor neuron disease. *Proc Natl Acad Sci U S A* **2010**, *107*, 13111-13116.

34. Reichenstein, I.; Eitan, C.; Diaz-Garcia, S.; Haim, G.; Magen, I.; Siany, A.; Hoye, M.L.; Rivkin, N.; Olender, T.; Toth, B., *et al.* Human genetics and neuropathology suggest a link between miR-218 and amyotrophic lateral sclerosis pathophysiology. *Sci Transl Med* **2019**, *11*, eaav5264.
35. Tung, Y.T.; Peng, K.C.; Chen, Y.C.; Yen, Y.P.; Chang, M.; Thams, S.; Chen, J.A. Mir-17 approximately 92 confers motor neuron subtype differential resistance to als-associated degeneration. *Cell Stem Cell* **2019**, *25*, 193-209 e197.
36. Chen, T.H.; Chen, J.A. Multifaceted roles of micrornas: From motor neuron generation in embryos to degeneration in spinal muscular atrophy. *eLife* **2019**, *8*, e50848.
37. Catapano, F.; Zaharieva, I.; Scoto, M.; Marrosu, E.; Morgan, J.; Muntoni, F.; Zhou, H. Altered levels of microrna-9, -206, and -132 in spinal muscular atrophy and their response to antisense oligonucleotide therapy. *Mol Ther Nucleic Acids* **2016**, *5*, e331.
38. Abiusi, E.; Infante, P.; Cagnoli, C.; Lospinoso Severini, L.; Pane, M.; Coratti, G.; Pera, M.C.; D'Amico, A.; Diano, F.; Novelli, A., *et al.* SMA-miRs (miR-181a-5p, -324-5p, and -451a) are overexpressed in spinal muscular atrophy skeletal muscle and serum samples *eLife* **2021**, *10*, e68054.
39. Wertz, M.H.; Winden, K.; Neveu, P.; Ng, S.Y.; Ercan, E.; Sahin, M. Cell-type-specific mir-431 dysregulation in a motor neuron model of spinal muscular atrophy. *Hum Mol Genet* **2016**, *25*, 2168-2181.
40. Verma, P.; Augustine, G.J.; Ammar, M.R.; Tashiro, A.; Cohen, S.M. A neuroprotective role for microrna mir-1000 mediated by limiting glutamate excitotoxicity. *Nat Neurosci* **2015**, *18*, 379-385.
41. McKenzie, A.J.; Hoshino, D.; Hong, N.H.; Cha, D.J.; Franklin, J.L.; Coffey, R.J.; Patton, J.G.; Weaver, A.M. Kras-mek signaling controls ago2 sorting into exosomes. *Cell Rep* **2016**, *15*, 978-987.
42. Mittelbrunn, M.; Gutierrez-Vazquez, C.; Villarroya-Beltri, C.; Gonzalez, S.; Sanchez-Cabo, F.; Gonzalez, M.A.; Bernad, A.; Sanchez-Madrid, F. Unidirectional transfer of microrna-loaded exosomes from t cells to antigen-presenting cells. *Nat Commun* **2011**, *2*, 282.
43. Shurtleff, M.J.; Temoche-Diaz, M.M.; Karfilis, K.V.; Ri, S.; Schekman, R. Y-box protein 1 is required to sort micrornas into exosomes in cells and in a cell-free reaction. *Elife* **2016**, *5*, e19276.

44. Tsai, Y.W.; Sung, H.H.; Li, J.C.; Yeh, C.Y.; Chen, P.Y.; Cheng, Y.J.; Chen, C.H.; Tsai, Y.C.; Chien, C.T. Glia-derived exosomal mir-274 targets sprouty in trachea and synaptic boutons to modulate growth and responses to hypoxia. *Proc Natl Acad Sci U S A* **2019**, *116*, 24651-24661.
45. Chen, T.H. Circulating micrnas as potential biomarkers and therapeutic targets in spinal muscular atrophy. *Ther Adv Neurol Disord* **2020**, *13*, 1756286420979954.
46. Wang, L.; Zhang, L. Circulating micrnas as diagnostic biomarkers for motor neuron disease. *Front Neurosci* **2020**, *14*, 354-354.
47. Viswambharan, V.; Thanseem, I.; Vasu, M.M.; Poovathinal, S.A.; Anitha, A. MiRNAs as biomarkers of neurodegenerative disorders. *Biomark Med* **2017**, *11*, 151-167.
48. Joilin, G.; Leigh, P.N.; Newbury, S.F.; Hafezparast, M. An overview of microRNAs as biomarkers of ALS. *Front Neurol* **2019**, *10*, 186.
49. Ravnik-Glavac, M.; Glavac, D. Circulating RNAs as potential biomarkers in amyotrophic lateral sclerosis. *Int J Mol Sci* **2020**, *21*, 1714.
50. Rao, P.; Benito, E.; Fischer, A. Micrnas as biomarkers for cns disease. *Front Mol Neurosci* **2013**, *6*, 39.
51. Saffari, A.; Cannet, C.; Blaschek, A.; Hahn, A.; Hoffmann, G.F.; Johannsen, J.; Kirsten, R.; Kockaya, M.; Kolker, S.; Muller-Felber, W., *et al.* ¹H-NMR-based metabolic profiling identifies non-invasive diagnostic and predictive urinary fingerprints in 5q spinal muscular atrophy. *Orphanet J Rare Dis* **2021**, *16*, 441.
52. Bishop, K.M.; Montes, J.; Finkel, R.S. Motor milestone assessment of infants with spinal muscular atrophy using the hammersmith infant neurological exam-part 2: Experience from a nusinersen clinical study. *Muscle Nerve* **2018**, *57*, 142-146.
53. Chang, S.H.; Su, Y.C.; Chang, M.; Chen, J.A. MicroRNAs mediate precise control of spinal interneuron populations to exert delicate sensory-to-motor outputs. *eLife* **2021**, *10*, e63768.
54. Wichterle, H.; Lieberam, I.; Porter, J.A.; Jessell, T.M. Directed differentiation of embryonic stem cells into motor neurons. *Cell* **2002**, *110*, 385-397.
55. Okita, K.; Matsumura, Y.; Sato, Y.; Okada, A.; Morizane, A.; Okamoto, S.; Hong, H.; Nakagawa, M.; Tanabe, K.; Tezuka, K., *et al.* A more efficient method to generate integration-free human ips cells. *Nat Methods* **2011**, *8*, 409-412.

56. Maury, Y.; Come, J.; Piskorowski, R.A.; Salah-Mohellibi, N.; Chevaleyre, V.; Peschanski, M.; Martinat, C.; Nedelec, S. Combinatorial analysis of developmental cues efficiently converts human pluripotent stem cells into multiple neuronal subtypes. *Nat Biotechnol* **2015**, *33*, 89-96.
57. Yen, Y.P.; Hsieh, W.F.; Tsai, Y.Y.; Lu, Y.L.; Liao, E.S.; Hsu, H.C.; Chen, Y.C.; Liu, T.C.; Chang, M.; Li, J., *et al.* Dlk1-dio3 locus-derived lncnas perpetuate postmitotic motor neuron cell fate and subtype identity. *Elife* **2018**, *7*, e38080.
58. Wang, T.H.; Huang, C.C.; Hung, J.H. Earrings: An efficient and accurate adapter trimmer entails no a priori adapter sequences. *Bioinformatics* **2021**, *37*:1846-1852.
59. Chou, M.T.; Han, B.W.; Hsiao, C.P.; Zamore, P.D.; Weng, Z.; Hung, J.H. Tailor: A computational framework for detecting non-templated tailing of small silencing rnas. *Nucleic Acids Res* **2015**, *43*, e109.
60. Frankish, A.; Diekhans, M.; Ferreira, A.M.; Johnson, R.; Jungreis, I.; Loveland, J.; Mudge, J.M.; Sisu, C.; Wright, J.; Armstrong, J., *et al.* Gencode reference annotation for the human and mouse genomes. *Nucleic Acids Res* **2019**, *47*, D766-D773.
61. Kozomara, A.; Birgaoanu, M.; Griffiths-Jones, S. Mirbase: From microRNA sequences to function. *Nucleic Acids Res* **2019**, *47*, D155-D162.
62. Shirak, A.; Grabherr, M.; Di Palma, F.; Lindblad-Toh, K.; Hulata, G.; Ron, M.; Kocher, T.D.; Seroussi, E. Identification of repetitive elements in the genome of oreochromis niloticus: Tilapia repeat masker. *Mar Biotechnol (NY)* **2010**, *12*, 121-125.
63. Huang da, W.; Sherman, B.T.; Lempicki, R.A. Systematic and integrative analysis of large gene lists using david bioinformatics resources. *Nat Protoc* **2009**, *4*, 44-57.
64. Tung, Y.T.; Lu, Y.L.; Peng, K.C.; Yen, Y.P.; Chang, M.; Li, J.; Jung, H.; Thams, S.; Huang, Y.P.; Hung, J.H., *et al.* Mir-17 approximately 92 governs motor neuron subtype survival by mediating nuclear pten. *Cell Rep* **2015**, *11*, 1305-1318.
65. Ramos, D.M.; d'Ydewalle, C.; Gabbeta, V.; Dakka, A.; Klein, S.K.; Norris, D.A.; Matson, J.; Taylor, S.J.; Zaworski, P.G.; Prior, T.W., *et al.* Age-dependent smn expression in disease-relevant tissue and implications for sma treatment. *J Clin Invest* **2019**, *129*, 4817-4831.

66. McGovern, V.L.; Gavrilina, T.O.; Beattie, C.E.; Burghes, A.H. Embryonic motor axon development in the severe sma mouse. *Hum Mol Genet* **2008**, *17*, 2900-2909.
67. Pomper, N.; Liu, Y.; Hoye, M.L.; Dougherty, J.D.; Miller, T.M. Cns microrna profiles: A database for cell type enriched microrna expression across the mouse central nervous system. *Sci Rep* **2020**, *10*, 4921.
68. Li, C.J.; Liao, E.S.; Lee, Y.H.; Huang, Y.Z.; Liu, Z.; Willems, A.; Garside, V.; McGlinn, E.; Chen, J.A.; Hong, T. Microrna governs bistable cell differentiation and lineage segregation via a noncanonical feedback. *Mol Syst Biol* **2021**, *17*, e9945.
69. Li, C.J.; Hong, T.; Tung, Y.T.; Yen, Y.P.; Hsu, H.C.; Lu, Y.L.; Chang, M.; Nie, Q.; Chen, J.A. Microrna filters hox temporal transcription noise to confer boundary formation in the spinal cord. *Nat Commun* **2017**, *8*, 14685.
70. Amin, N.D.; Senturk, G.; Costaguta, G.; Driscoll, S.; O'Leary, B.; Bonanomi, D.; Pfaff, S.L. A hidden threshold in motor neuron gene networks revealed by modulation of mir-218 dose. *Neuron* **2021**, *109*, 3252-3267 e3256.
71. Thiebes, K.P.; Nam, H.; Cambronne, X.A.; Shen, R.; Glasgow, S.M.; Cho, H.H.; Kwon, J.S.; Goodman, R.H.; Lee, J.W.; Lee, S., *et al.* Mir-218 is essential to establish motor neuron fate as a downstream effector of isl1-lhx3. *Nat Commun* **2015**, *6*, 7718.
72. Magen, I.; Aharoni, S.; Yacovzada, N.S.; Tokatly Latzer, I.; Alves, C.R.R.; Sagi, L.; Fattal-Valevski, A.; Swoboda, K.J.; Katz, J.; Bruckheimer, E., *et al.* Muscle micrnas in the cerebrospinal fluid predict clinical response to nusinersen therapy in type II and type III spinal muscular atrophy patients. *Eur J Neurol* **2022**, *29*, 2420-2430.
73. Sances, S.; Ho, R.; Vatine, G.; West, D.; Laperle, A.; Meyer, A.; Godoy, M.; Kay, P.S.; Mandefro, B.; Hatata, S., *et al.* Human iPSC-derived endothelial cells and microengineered organ-chip enhance neuronal development. *Stem Cell Reports* **2018**, *10*, 1222-1236.
74. Fuller, H.R.; Mandefro, B.; Shirran, S.L.; Gross, A.R.; Kaus, A.S.; Botting, C.H.; Morris, G.E.; Sareen, D. Spinal muscular atrophy patient ipsc-derived motor neurons have reduced expression of proteins important in neuronal development. *Front Cell Neurosci* **2015**, *9*, 506.
75. Le, T.T.; Pham, L.T.; Butchbach, M.E.; Zhang, H.L.; Monani, U.R.; Coover, D.D.; Gavrilina, T.O.; Xing, L.; Bassell, G.J.; Burghes, A.H. Smndelta7, the major product of the centromeric survival motor neuron (smn2) gene, extends

- survival in mice with spinal muscular atrophy and associates with full-length smn. *Hum Mol Genet* **2005**, *14*, 845-857.
76. Hermeking, H. The mir-34 family in cancer and apoptosis. *Cell Death Differ* **2010**, *17*, 193-199.
77. Simon, C.M.; Dai, Y.; Van Alstyne, M.; Koutsoumpa, C.; Pagiazitis, J.G.; Chalif, J.I.; Wang, X.; Rabinowitz, J.E.; Henderson, C.E.; Pellizzoni, L., *et al.* Converging mechanisms of p53 activation drive motor neuron degeneration in spinal muscular atrophy. *Cell Rep* **2017**, *21*, 3767-3780.
78. Bowerman, M.; Murray, L.M.; Boyer, J.G.; Anderson, C.L.; Kothary, R. Fasudil improves survival and promotes skeletal muscle development in a mouse model of spinal muscular atrophy. *BMC Med* **2012**, *10*, 24.
79. Courtney, N.L.; Mole, A.J.; Thomson, A.K.; Murray, L.M. Reduced p53 levels ameliorate neuromuscular junction loss without affecting motor neuron pathology in a mouse model of spinal muscular atrophy. *Cell Death Dis* **2019**, *10*, 515.
80. Tsai, M.S.; Chiu, Y.T.; Wang, S.H.; Hsieh-Li, H.M.; Lian, W.C.; Li, H. Abolishing bax-dependent apoptosis shows beneficial effects on spinal muscular atrophy model mice. *Mol Ther* **2006**, *13*, 1149-1155.
81. Motyl, A.A.L.; Faller, K.M.E.; Groen, E.J.N.; Kline, R.A.; Eaton, S.L.; Ledahawsky, L.M.; Chaytow, H.; Lamont, D.J.; Wishart, T.M.; Huang, Y.T., *et al.* Pre-natal manifestation of systemic developmental abnormalities in spinal muscular atrophy. *Hum Mol Genet* **2020**, *29*, 2674-2683.
82. Kong, L.; Wang, X.; Choe, D.W.; Polley, M.; Burnett, B.G.; Bosch-Marce, M.; Griffin, J.W.; Rich, M.M.; Sumner, C.J. Impaired synaptic vesicle release and immaturity of neuromuscular junctions in spinal muscular atrophy mice. *J Neurosci* **2009**, *29*, 842-851.
83. Kariya, S.; Park, G.H.; Maeno-Hikichi, Y.; Leykekhman, O.; Lutz, C.; Arkovitz, M.S.; Landmesser, L.T.; Monani, U.R. Reduced smn protein impairs maturation of the neuromuscular junctions in mouse models of spinal muscular atrophy. *Hum Mol Genet* **2008**, *17*, 2552-2569.
84. Mentis, G.Z.; Blivis, D.; Liu, W.; Drobac, E.; Crowder, M.E.; Kong, L.; Alvarez, F.J.; Sumner, C.J.; O'Donovan, M.J. Early functional impairment of sensory-motor connectivity in a mouse model of spinal muscular atrophy. *Neuron* **2011**, *69*, 453-467.
85. Zhang, Z.; Pinto, A.M.; Wan, L.; Wang, W.; Berg, M.G.; Oliva, I.; Singh, L.N.; Dengler, C.; Wei, Z.; Dreyfuss, G. Dysregulation of synaptogenesis

- genes antecedes motor neuron pathology in spinal muscular atrophy. *Proceedings of the National Academy of Sciences of the United States of America* **2013**, *110*, 19348-19353.
86. Jangi, M.; Fleet, C.; Cullen, P.; Gupta, S.V.; Mekhoubad, S.; Chiao, E.; Allaire, N.; Bennett, C.F.; Rigo, F.; Krainer, A.R., *et al.* Smn deficiency in severe models of spinal muscular atrophy causes widespread intron retention and DNA damage. *Proc Natl Acad Sci U S A* **2017**, *114*, E2347-E2356.
 87. Baumer, D.; Lee, S.; Nicholson, G.; Davies, J.L.; Parkinson, N.J.; Murray, L.M.; Gillingwater, T.H.; Ansorge, O.; Davies, K.E.; Talbot, K. Alternative splicing events are a late feature of pathology in a mouse model of spinal muscular atrophy. *PLoS Genet* **2009**, *5*, e1000773.
 88. Zucchi, E.; Bonetto, V.; Soraru, G.; Martinelli, I.; Parchi, P.; Liguori, R.; Mandrioli, J. Neurofilaments in motor neuron disorders: Towards promising diagnostic and prognostic biomarkers. *Mol Neurodegener* **2020**, *15*, 58.
 89. De Vivo, D.C.; Bertini, E.; Swoboda, K.J.; Hwu, W.L.; Crawford, T.O.; Finkel, R.S.; Kirschner, J.; Kuntz, N.L.; Parsons, J.A.; Ryan, M.M., *et al.* Nusinersen initiated in infants during the presymptomatic stage of spinal muscular atrophy: Interim efficacy and safety results from the phase 2 nurture study. *Neuromuscul Disord* **2019**, *29*, 842-856.
 90. Darras, B.T.; Crawford, T.O.; Finkel, R.S.; Mercuri, E.; De Vivo, D.C.; Oskoui, M.; Tizzano, E.F.; Ryan, M.M.; Muntoni, F.; Zhao, G., *et al.* Neurofilament as a potential biomarker for spinal muscular atrophy. *Ann Clin Transl Neurol* **2019**, *6*, 932-944.
 91. Winter, B.; Guenther, R.; Ludolph, A.C.; Hermann, A.; Otto, M.; Wurster, C.D. Neurofilaments and tau in csf in an infant with sma type 1 treated with nusinersen. *J Neurol Neurosurg Psychiatry* **2019**, *90*, 1068-1069.
 92. Farrar, M.A.; Muntoni, F.; Sumner, C.J.; Crawford, T.O.; Finkel, R.S.; Mercuri, E.; Jiang, X.; Sohn, J.; Petrillo, M.; Garafalo, S., *et al.* Plasma phosphorylated neurofilament heavy chain (pnf-h) level is associated with future motor function in nusinersen-treated individuals with later-onset spinal muscular atrophy (sma) (2248). *Neurology* **2021**, *96*.
 93. Hensel, N.; Kubinski, S.; Claus, P. The Need for SMN-Independent Treatments of Spinal Muscular Atrophy (SMA) to Complement SMN-Enhancing Drugs. *Front Neurol* **2020**, *11*, 45.
 94. Boido, M.; Vercelli, A. Neuromuscular junctions as key contributors and therapeutic targets in spinal muscular atrophy. *Front Neuroanat* **2016**, *10*, 6.

95. Chen, J.A.; Wichterle, H. Apoptosis of limb innervating motor neurons and erosion of motor pool identity upon lineage specific *dicer* inactivation. *Front Neurosci* **2012**, *6*, 69.
96. Nelson, P.T.; Hatzigeorgiou, A.G.; Mourelatos, Z. Mirnp:Mrna association in polyribosomes in a human neuronal cell line. *RNA* **2004**, *10*, 387-394.
97. Kong, L.; Valdivia, D.O.; Simon, C.M.; Hassinan, C.W.; Delestree, N.; Ramos, D.M.; Park, J.H.; Pilato, C.M.; Xu, X.; Crowder, M., *et al.* Impaired prenatal motor axon development necessitates early therapeutic intervention in severe SMA. *Sci Transl Med* **2021**, *13*, eabb6871.
98. Shorrock, H.K.; Gillingwater, T.H.; Groen, E.J.N. Molecular mechanisms underlying sensory-motor circuit dysfunction in *sma*. *Front Mol Neurosci* **2019**, *12*, 59.
99. Fletcher, E.V.; Simon, C.M.; Pagiazitis, J.G.; Chalif, J.I.; Vukojicic, A.; Drobnac, E.; Wang, X.; Mentis, G.Z. Reduced sensory synaptic excitation impairs motor neuron function via *kv2.1* in spinal muscular atrophy. *Nat Neurosci* **2017**, *20*, 905-916.
100. Ling, K.K.; Lin, M.Y.; Zingg, B.; Feng, Z.; Ko, C.P. Synaptic defects in the spinal and neuromuscular circuitry in a mouse model of spinal muscular atrophy. *PLoS One* **2010**, *5*, e15457.
101. Shorrock, H.K.; van der Hoorn, D.; Boyd, P.J.; Llayero Hurtado, M.; Lamont, D.J.; Wirth, B.; Sleight, J.N.; Schiavo, G.; Wishart, T.M.; Groen, E.J.N., *et al.* UBA1/GARS-dependent pathways drive sensory-motor connectivity defects in spinal muscular atrophy. *Brain* **2018**, *141*, 2878-2894.
102. Buettner, J.M.; Sime Longang, J.K.; Gerstner, F.; Apel, K.S.; Blanco-Redondo, B.; Sowoidnich, L.; Janzen, E.; Langenhan, T.; Wirth, B.; Simon, C.M. Central synaptopathy is the most conserved feature of motor circuit pathology across spinal muscular atrophy mouse models. *iScience* **2021**, *24*, 103376.
103. McNeill, E.M.; Warinner, C.; Alkins, S.; Taylor, A.; Heggeness, H.; DeLuca, T.F.; Fulga, T.A.; Wall, D.P.; Griffith, L.C.; Van Vactor, D. The conserved microRNA *mir-34* regulates synaptogenesis via coordination of distinct mechanisms in presynaptic and postsynaptic cells. *Nat Commun* **2020**, *11*, 1092.
104. Kaifer, K.A.; Villalon, E.; O'Brien, B.S.; Sison, S.L.; Smith, C.E.; Simon, M.E.; Marquez, J.; O'Day, S.; Hopkins, A.E.; Neff, R., *et al.* AAV9-mediated delivery of *mir-23a* reduces disease severity in *smn2b/-sma* model mice. *Hum Mol Genet* **2019**, *28*, 3199-3210.

105. Hoye, M.L.; Regan, M.R.; Jensen, L.A.; Lake, A.M.; Reddy, L.V.; Vidensky, S.; Richard, J.P.; Maragakis, N.J.; Rothstein, J.D.; Dougherty, J.D., *et al.* Motor neuron-derived micrnas cause astrocyte dysfunction in amyotrophic lateral sclerosis. *Brain* **2018**, *141*, 2561-2575.
106. Mercuri, E.; Pera, M.C.; Scoto, M.; Finkel, R.; Muntoni, F. Spinal muscular atrophy - insights and challenges in the treatment era. *Nature reviews. Neurology* **2020**.
107. Messina, S.; Sframeli, M. New treatments in spinal muscular atrophy: Positive results and new challenges. *J Clin Med* **2020**, *9*:2222.
108. De Paola, E.; Verdile, V.; Paronetto, M.P. Dysregulation of microrna metabolism in motor neuron diseases: Novel biomarkers and potential therapeutics. *Noncoding RNA Res* **2019**, *4*, 15-22.
109. Main, M.; Kairon, H.; Mercuri, E.; Muntoni, F. The hammersmith functional motor scale for children with spinal muscular atrophy: A scale to test ability and monitor progress in children with limited ambulation. *Eur J Paediatr Neurol* **2003**, *7*, 155-159.
110. Saffari, A.; Kolker, S.; Hoffmann, G.F.; Weiler, M.; Ziegler, A. Novel challenges in spinal muscular atrophy - how to screen and whom to treat? *Ann Clin Transl Neurol* **2019**, *6*, 197-205.
111. Tseng, Y.-H.; Chen, T.-H. Care for patients with neuromuscular disorders in the covid-19 pandemic era. *Front Neurol* **2021**, *12*, 607790.
112. Kolb, S.J.; Coffey, C.S.; Yankey, J.W.; Krosschell, K.; Arnold, W.D.; Rutkove, S.B.; Swoboda, K.J.; Reyna, S.P.; Sakonju, A.; Darras, B.T., *et al.* Natural history of infantile-onset spinal muscular atrophy. *Ann Neurol* **2017**, *82*, 883-891.
113. Navarrete-Opazo, A.; Garrison, S.; Waite, M. Molecular biomarkers for spinal muscular atrophy: A systematic review. *Neurol Clin Pract* **2021**, *11*, e524-e536.
114. Gidaro, T.; Servais, L. Nusinersen treatment of spinal muscular atrophy: Current knowledge and existing gaps. *Dev Med Child Neurol* **2019**, *61*, 19-24.
115. Kessler, T.; Latzer, P.; Schmid, D.; Warnken, U.; Saffari, A.; Ziegler, A.; Kollmer, J.; Mohlenbruch, M.; Ulfert, C.; Herweh, C., *et al.* Cerebrospinal fluid proteomic profiling in nusinersen-treated patients with spinal muscular atrophy. *J Neurochem* **2020**, *153*, 545-548.
116. Olsson, B.; Alberg, L.; Cullen, N.C.; Michael, E.; Wahlgren, L.; Kroksmark, A.K.; Rostasy, K.; Blennow, K.; Zetterberg, H.; Tulinus, M. NFL is a marker

- of treatment response in children with sma treated with nusinersen. *J Neurol* **2019**, 266, 2129-2136.
117. Yuan, A.; Rao, M.V.; Veeranna; Nixon, R.A. Neurofilaments and neurofilament proteins in health and disease. *Cold Spring Harb Perspect Biol* **2017**, 9, a018309.
 118. Spicer, C.; Lu, C.H.; Catapano, F.; Scoto, M.; Zaharieva, I.; Malaspina, A.; Morgan, J.E.; Greensmith, L.; Muntoni, F.; Zhou, H. The altered expression of neurofilament in mouse models and patients with spinal muscular atrophy. *Ann Clin Transl Neurol* **2021**, 8:866-876.
 119. Wurster, C.D.; Gunther, R.; Steinacker, P.; Dreyhaupt, J.; Wollinsky, K.; Uzelac, Z.; Witzel, S.; Kocak, T.; Winter, B.; Koch, J.C., *et al.* Neurochemical markers in csf of adolescent and adult sma patients undergoing nusinersen treatment. *Ther Adv Neurol Disord* **2019**, 12, 1756286419846058.
 120. Totzeck, A.; Stolte, B.; Kizina, K.; Bolz, S.; Schlag, M.; Thimm, A.; Kleinschmitz, C.; Hagenacker, T. Neurofilament heavy chain and tau protein are not elevated in cerebrospinal fluid of adult patients with spinal muscular atrophy during loading with nusinersen. *Int J Mol Sci* **2019**, 20, 5397.
 121. Faravelli, I.; Meneri, M.; Saccomanno, D.; Velardo, D.; Abati, E.; Gagliardi, D.; Parente, V.; Petrozzi, L.; Ronchi, D.; Stocchetti, N., *et al.* Nusinersen treatment and cerebrospinal fluid neurofilaments: An explorative study on spinal muscular atrophy type 3 patients. *J Cell Mol Med* **2020**, 24, 3034-3039.
 122. Toivonen, J.M.; Manzano, R.; Olivan, S.; Zaragoza, P.; Garcia-Redondo, A.; Osta, R. MicroRNA-206: a potential circulating biomarker candidate for amyotrophic lateral sclerosis. *PLoS One* **2014**, 9, e89065.
 123. Alexander, M.S.; Kunkel, L.M. Skeletal muscle micrornas: Their diagnostic and therapeutic potential in human muscle diseases. *J Neuromuscul Dis* **2015**, 2, 1-11.
 124. Perry, M.M.; Muntoni, F. Noncoding RNAs and duchenne muscular dystrophy. *Epigenomics* **2016**, 8, 1527-1537.
 125. Israeli, D.; Poupiot, J.; Amor, F.; Charton, K.; Lostal, W.; Jeanson-Leh, L.; Richard, I. Circulating miRNAs are generic and versatile therapeutic monitoring biomarkers in muscular dystrophies. *Sci Rep* **2016**, 6, 28097.
 126. Bonanno, S.; Marcuzzo, S.; Malacarne, C.; Giagnorio, E.; Masson, R.; Zanin, R.; Arnoldi, M.T.; Andreetta, F.; Simoncini, O.; Venerando, A., *et al.* Circulating myomirs as potential biomarkers to monitor response to nusinersen in pediatric SMA patients. *Biomedicines* **2020**, 8, 21.

127. Zaharieva, I.T.; Scoto, M.; Aragon-Gawinska, K.; Ridout, D.; Doreste, B.; Servais, L.; Muntoni, F.; Zhou, H. Response of plasma microRNAs to nusinersen treatment in patients with SMA. *Ann Clin Transl Neurol* **2022**, *9*, 1011-1026.
128. D'Silva, A.M.; Kariyawasam, D.; Venkat, P.; Mayoh, C.; Farrar, M.A. Identification of novel csf-derived miRNAs in treated paediatric onset spinal muscular atrophy: An exploratory study. *Pharmaceutics* **2023**, *15*, 170.
129. Alves, C.R.R.; Petrillo, M.; Spellman, R.; Garner, R.; Zhang, R.; Kiefer, M.; Simeone, S.; Sohn, J.; Eichelberger, E.J.; Rodrigues, E., *et al.* Implications of circulating neurofilaments for spinal muscular atrophy treatment early in life: A case series. *Mol Ther Methods Clin Dev* **2021**, *23*, 524-538.
130. Tisdale, S.; Pellizzoni, L. Disease mechanisms and therapeutic approaches in spinal muscular atrophy. *J Neurosci* **2015**, *35*, 8691-8700.
131. Tozawa, T.; Kasai, T.; Tatebe, H.; Shiomi, K.; Nishio, H.; Tokuda, T.; Chiyonobu, T. Intrathecal nusinersen treatment after ventriculo-peritoneal shunt placement: A case report focusing on the neurofilament light chain in cerebrospinal fluid. *Brain Dev* **2020**, *42*, 311-314.
132. Poirier, A.; Weetall, M.; Heinig, K.; Bucheli, F.; Schoenlein, K.; Alsenz, J.; Bassett, S.; Ullah, M.; Senn, C.; Ratni, H., *et al.* Risdiplam distributes and increases smn protein in both the central nervous system and peripheral organs. *Pharmacol Res Perspect* **2018**, *6*, e00447.
133. Alves, C.R.R.; Zhang, R.; Johnstone, A.J.; Garner, R.; Eichelberger, E.J.; Lepez, S.; Yi, V.; Stevens, V.; Poxson, R.; Schwartz, R., *et al.* Whole blood survival motor neuron protein levels correlate with severity of denervation in spinal muscular atrophy. *Muscle Nerve* **2020**, *62*, 351-357.
134. Alves, C.R.R.; Zhang, R.; Johnstone, A.J.; Garner, R.; Nwe, P.H.; Siranosian, J.J.; Swoboda, K.J. Serum creatinine is a biomarker of progressive denervation in spinal muscular atrophy. *Neurology* **2020**, *94*, e921-e931.
135. Deutsch, L.; Osredkar, D.; Plavec, J.; Stres, B. Spinal Muscular Atrophy after Nusinersen Therapy: Improved Physiology in Pediatric Patients with No Significant Change in Urine, Serum, and Liquor ¹H-NMR Metabolomes in Comparison to an Age-Matched, Healthy Cohort. *Metabolites* **2021**, *11*, 206.
136. Freigang, M.; Wurster, C.D.; Hagenacker, T.; Stolte, B.; Weiler, M.; Kamm, C.; Schreiber-Katz, O.; Osmanovic, A.; Petri, S.; Kowski, A., *et al.* Serum creatine kinase and creatinine in adult spinal muscular atrophy under nusinersen treatment. *Ann Clin Transl Neurol* **2021**, *8*, 1049-1063.

137. Johannsen, J.; Weiss, D.; Daubmann, A.; Schmitz, L.; Denecke, J. Evaluation of putative CSF biomarkers in paediatric spinal muscular atrophy (SMA) patients before and during treatment with nusinersen. *J Cell Mol Med.* **2021**, *25*, 8419-8431.





Appendix

Fig. S1

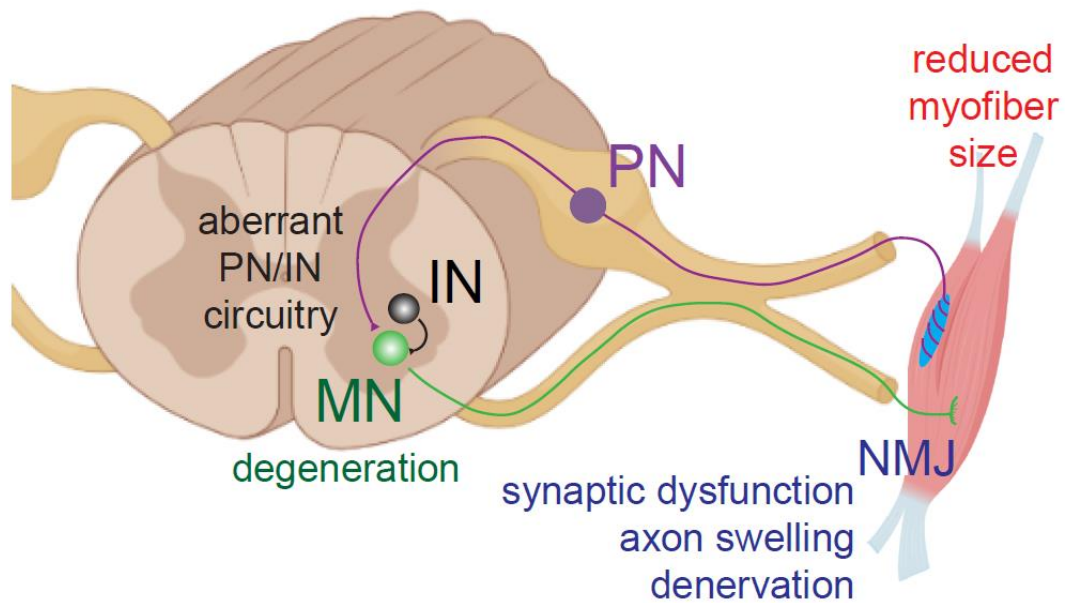
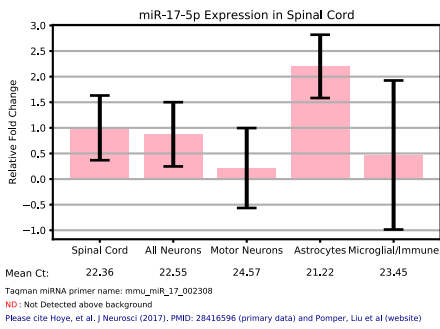


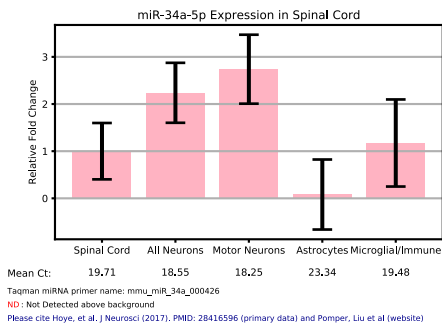
Figure S1. Summary of known possible causes of selective motor neuron degeneration in SMA. PN: proprioceptive sensory neurons; IN: interneuron; MN: motor neuron; NMJ: neuromuscular junction. Adapted from the previous study of Tisdale et al.[130].

Fig S2

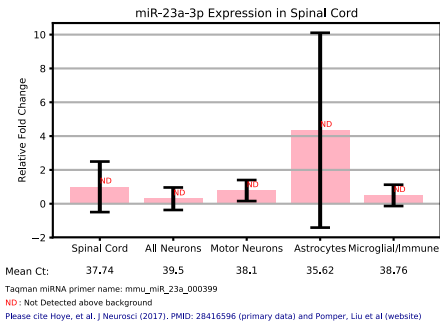
A



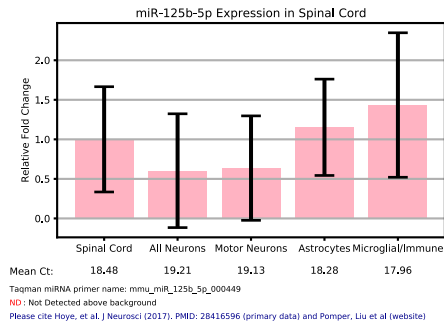
E



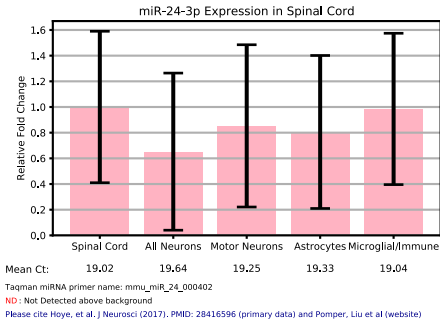
B



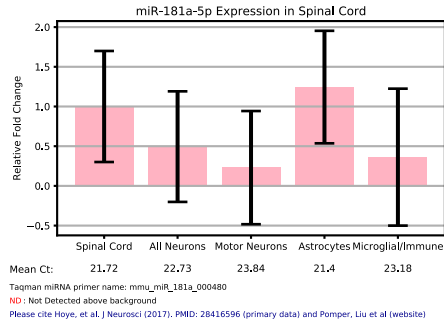
F



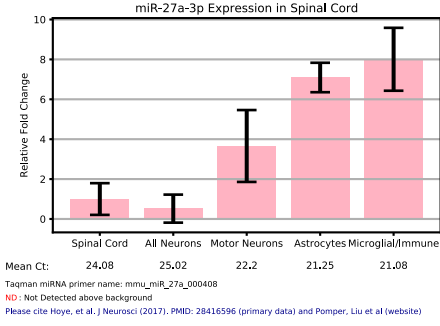
C



G



D



H

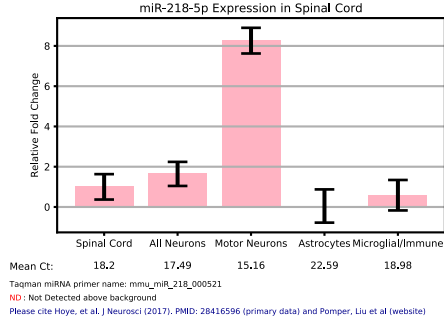


Figure S2. Expression profiles of the candidate miRNAs.

Expression profiles for the indicated miRNAs in mouse spinal cord from available data sources (<https://mirna.wustl.edu>).



Fig. S3

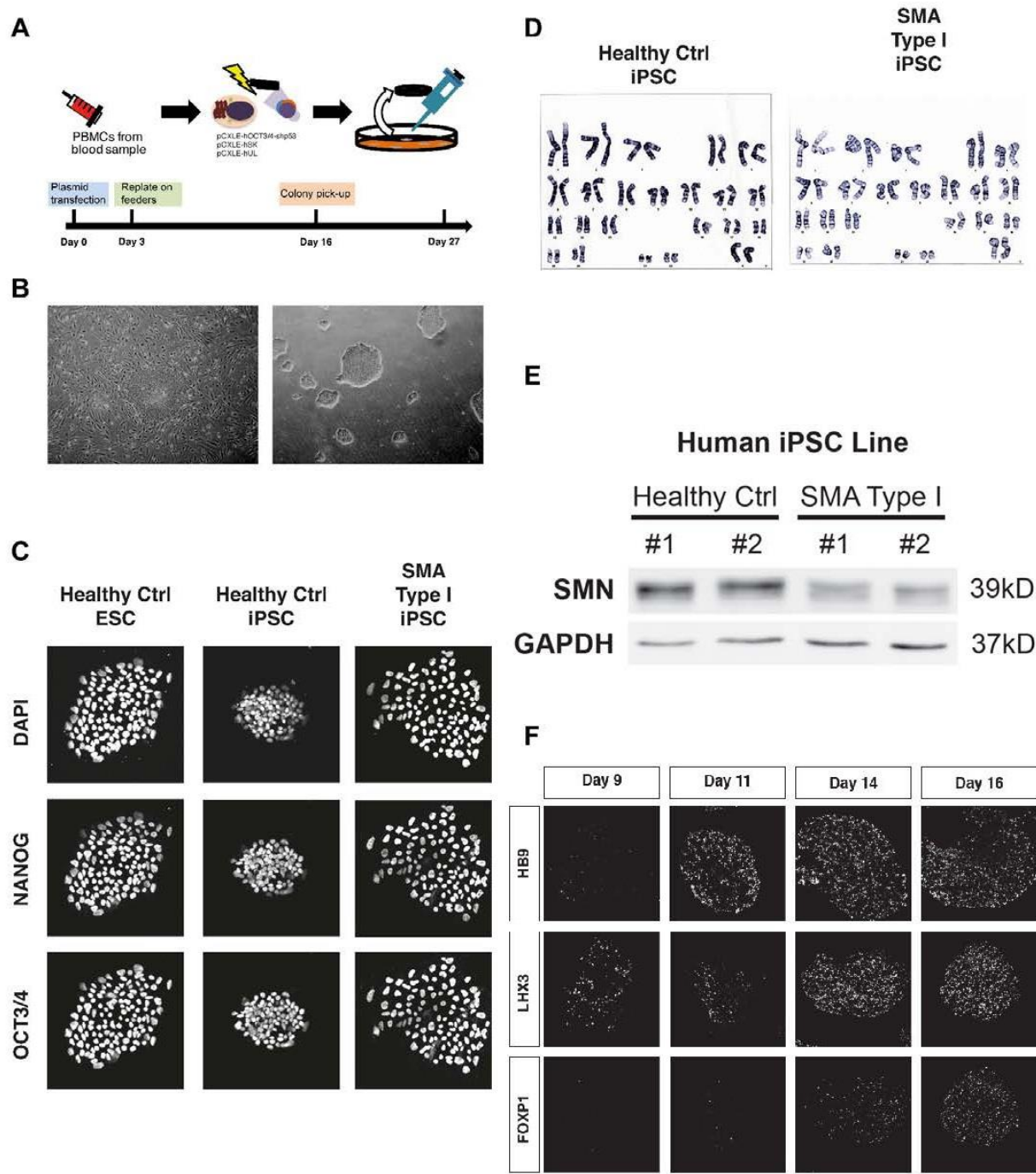


Figure S3. Establishment and characterization of induced pluripotent stem cells (iPSCs) from type I SMA patients.

(A) Schematic illustration of the SMA iPSC derivation process. Peripheral blood mononuclear cells (PBMCs) were reprogrammed into iPSCs through transient expression of OCT4, SOX2, KLF4, LIN28, and SHP53 via electroporation. Colonies with an ESC-like morphology were then picked at day 16. (B) The iPSCs formed ESC-like colonies under both feeder-dependent and feeder-free conditions. (C) Pluripotency markers NANOG and OCT3/4 are expressed in healthy controls and SMA iPSCs. (D) Karyotypes are normal in both control and type I SMA iPSC lines. (E) Western blotting reveals compromised SMN protein levels in SMA iPSCs relative to healthy control iPSCs, indicating that patient-derived iPSCs could recapitulate the molecular pathology of SMA. (F) MN markers HB9, LHX3 and FOXP1 are expressed in healthy controls and SMA iPSC derived MNs.

Fig. S4

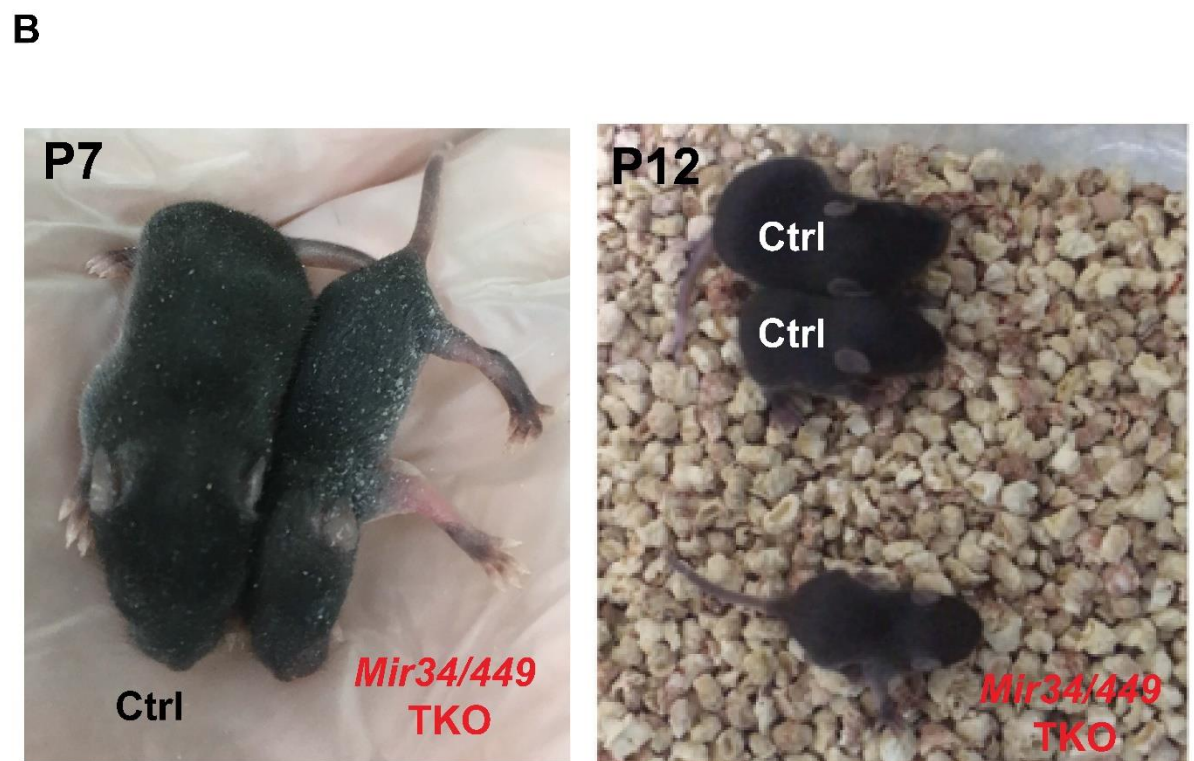
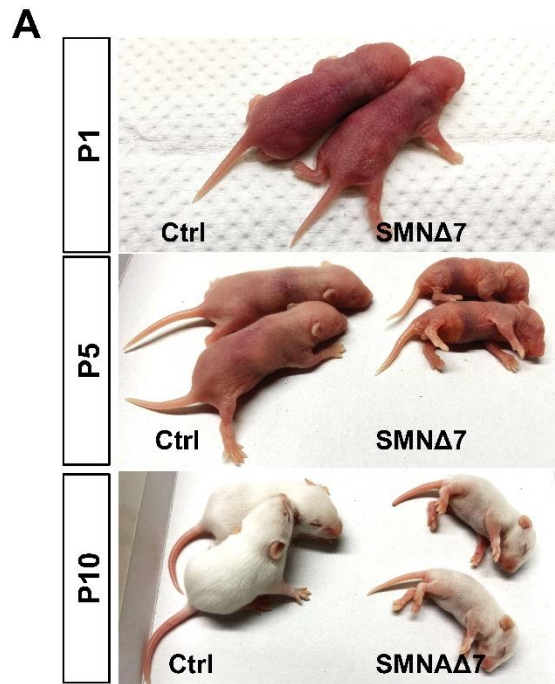


Figure S4. Severe disease phenotype of SMN Δ 7 and *Mir34/449* TKO mice.

Representative images illustrating the severe disease phenotype of (A) SMN Δ 7 mice at P1, P5 and P10, and (B) *Mir34/449* TKO mice at early postnatal stages demonstrating their smaller body size compared to the littermate Ctrl group.



Fig. S5

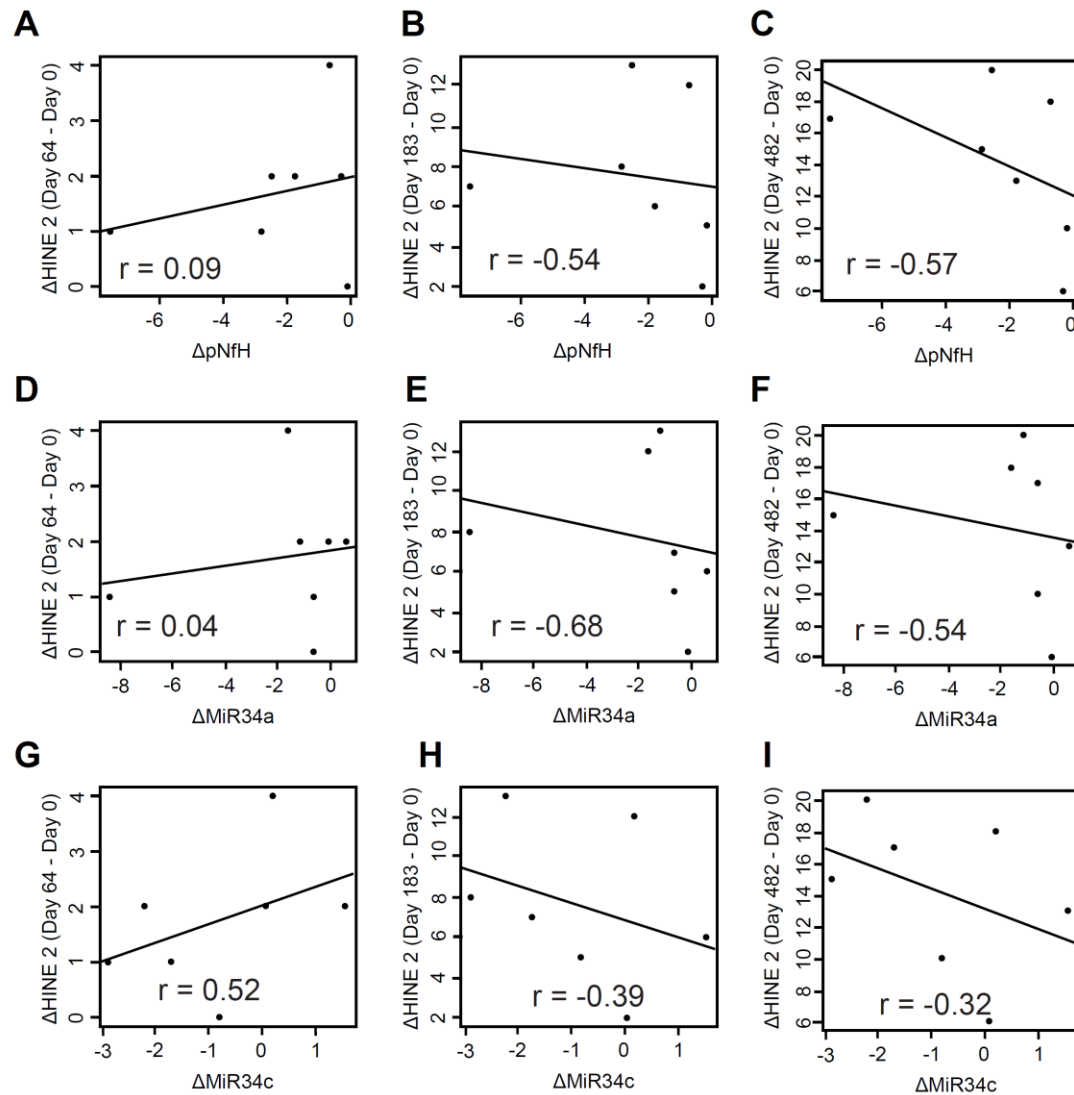


Figure S5. Correlation between HINE2 scores and altered miRNA expression in CSF.

(A-I) Correlation between changing HINE-2 scores over the nusinersen treatment time-course and the change in pNfH (A-C), MiR34a (D-F), and MiR34c (G-I) levels in CSF after two months (Day 64) of nusinersen treatment. Coefficients (r) lower than -0.5 indicate a strong inverse correlation.

Table S1. Molecular biomarkers in monitoring treatment response to SMA novel therapies					
Biomarker	Source of production	Advantages and Feasibilities	Applications in approved SMA therapies	Limitations	References
pNF-H	A content of filling axonal caliber which is secreted by neuron following injury	<ol style="list-style-type: none"> 1. High neuronal specificity, which may reliably represent the status of M.N. rescue after therapy 2. Highly sensitive in detecting the earliest stages of M.N. degeneration, helping guide decisions in the presymptomatic patient regarding the timing of start treatment. 	<ol style="list-style-type: none"> 1. Plasma pNF-H declined more rapidly in the nusinersen-treated cohort with severe infantile SMA. 2. Declined CSF pNF-H showed declined levels after nusinersen treatment. 	<ol style="list-style-type: none"> 1. Because of highly neuronal specificity, pNF-H may not reflect the condition of extra-MN tissues such as muscles and NMJ, which also contributes to SMA treatment outcomes. 2. Less sensitive in assessing treatment response of chronic forms of SMA patients. 3. With a half-life up to 8 months, peripheral pNF-H levels may only reflect CNS condition occurring weeks or months earlier. 	[90,91,118, 120,121,131]
miRNAs	Small non-encoding RNAs	<ol style="list-style-type: none"> 1. Clinically detectable in many biofluids 	<ol style="list-style-type: none"> 1. Altered miR-132 levels in spinal cord, muscle, and 	<ol style="list-style-type: none"> 1. Relatively small size and low efficiency of 	[37,72,126-128]

	(~20 nt) act as splicing modulators affecting different levels of SMN expression	<p>with relative stabilities (CSF, serum/plasma, saliva, and urine)</p> <p>2. Due to versatile roles in regulating MNs, muscles, and NMJ involved in SMA pathogenesis, different tissue-specific miRNAs can help monitor therapeutic response.</p>	<p>serum of SMA mice after morpholino ASO treatment.</p> <p>2. Significantly decreased serum miR-133a in SMA patients after nusinersen treatment.</p>	<p>extracting miRNAs fragments limit their sensitivity and specificity for quantitative detection</p> <p>2. The altered miRNAs level is not specific to MN diseases (e.g., miR-9 can be differentially expressed in Huntington's disease and Parkinson's disease).</p> <p>3. The variable levels among different tissue sample associated with mechanism of miRNA production and transportation are still unclear.</p>	
SMN	SMN mRNA and proteins are transcribed and translated, respectively, from	<p>1. Changes in level may reflect the productive efficacy of currently approved</p>	<p>1. Increased SMN expressions in blood and CSF of SMA patients after risdiplam treatment.</p> <p>2. Increased SMN protein in</p>	<p>1. Several studies suggested that SMN expressions were not satisfactorily correlated with</p>	[65,112,132,133]

	variable <i>SMN2</i> copies retained in SMA patients	<p>SMN-dependent therapies.</p> <ol style="list-style-type: none"> 2. Easy accessibility in different biofluids, especially blood 3. Useful in investigating the systemic response to MN-targeted therapies. 	<p>spinal M.N.s of five SMA infants after nusinersen treatment.</p> <ol style="list-style-type: none"> 3. Neither nusinersen nor gene therapy altered SMN levels in patients' whole blood. 	<p><i>SMN2</i> copy number, disease severity, or motor function, possibly related to post-transcriptional modulation.</p> <ol style="list-style-type: none"> 2. As SMN ubiquitously present in various tissues, tissue-dependent expression may cause inconsistency between peripheral (blood) and central (CSF) specimens. 3. Maybe less useful in evaluating SMN-independent therapies (e.g., muscle- or NMJ-targeted therapies). 	
--	--	--	---	---	--

				<p>4. Less sensitive in evaluating treatment response of elder and milder forms of SMA patients.</p> <p>5. The baseline and change level of SMN may vary with age.</p>	
Creatinine	<p>A metabolic waste produced by creatinine kinase system and a marker of muscle mass, previously shown to correlate with disease severity in several MN diseases.</p>	<p>1. Easy accessibility from blood and cost-effective as a routine laboratory checked item.</p> <p>2. Showing a significant correlation with SMA type, <i>SMN2</i> copy number, motor function, and status of denervation. [134]</p>	<p>1. Decreased creatine kinase and increased creatinine suggested a positive response to nusinersen treatment.</p> <p>2. Urine creatinine of SMA patients did not change significantly in response to nusinersen treatment.</p>	<p>1. Creatinine production varies between individuals and over time in association with changes in muscle mass and diet.</p> <p>2. Lacking SMN is known to cause hepatic or renal tubular dysfunction, which may affect serum creatinine levels.</p> <p>3. Urine creatinine level did not change significantly in response to nusinersen therapy.</p>	[134-136]

Tau	A microtubule-associated structure protein involved in regulating intracellular trafficking and signal transduction of neurons.	Elevated tau in the CSF represent neuron damage and progression, in various neurodegenerative disease, but also found in SMA.	<ol style="list-style-type: none"> 1. Elevated CSF tau protein in a type I SMA infant, and decreased after nusinersen treatment. 2. In another larger cohort study, CSF tau levels significantly decreased in SMA type I and 2 patients from baseline to 10 months of nusinersen treatment. 	<ol style="list-style-type: none"> 1. Similar to pNF-H, tau may have less sensitivity to assess nusinersen treatment response in types 2/3 SMA patients. 2. Tau production is not specific to MN, and mostly related to cortical neurons. 	[91,120,137]
SMA: spinal muscular atrophy, SMN: survival motor neuron, MN: motor neuron, CSF: cerebrospinal fluid, pNF-H: phosphorylated neurofilament heavy chain, miRNA: microRNA, NMJ: neuromuscular junction					

